Ryerson University
Digital Commons @ Ryerson

Theses and dissertations

1-1-2010

Coverage Based Tool-Path Planning For Automated Polishing Using Contact Mechanics Theory

Michael Rososhansky
Ryerson University

Follow this and additional works at: http://digitalcommons.ryerson.ca/dissertations

 Part of the Aerospace Engineering Commons

Recommended Citation
Rososhansky, Michael, "Coverage Based Tool-Path Planning For Automated Polishing Using Contact Mechanics Theory" (2010). *Theses and dissertations*. Paper 1621.

This Thesis is brought to you for free and open access by Digital Commons @ Ryerson. It has been accepted for inclusion in Theses and dissertations by an authorized administrator of Digital Commons @ Ryerson. For more information, please contact bcameron@ryerson.ca.

COVERAGE BASED TOOL-PATH PLANNING FOR AUTOMATED POLISHING USING CONTACT MECHANICS THEORY

By

Michael Rososhansky
Bachelor of Engineering
Ryerson University
Toronto, Ontario, Canada

A thesis
presented to Ryerson University
in partial fulfillment of the
requirements for the degree of
Master of Applied Science
in the Program of
Aerospace Engineering

Toronto, Ontario, Canada, 2010

©Michael Rososhansky, 2010

Author's Declaration

I hereby declare that I am the sole author of this thesis or dissertation.

I authorize Ryerson University to lend this thesis or dissertation to other institutions or individuals for the purpose of scholarly research.

_____

I further authorize Ryerson University to reproduce this thesis or dissertation by photocopying or by other means, in total or in part, at the request of other institutions or individuals for the purpose of scholarly research.

_____

Abstract

COVERAGE BASED TOOL-PATH PLANNING FOR AUTOMATED POLISHING USING CONTACT MECHANICS THEORY

Michael Rososhansky

A thesis for the degree of

Master of Applied Science, 2010

Department of Aerospace Engineering, Ryerson University

Presented in this thesis is a method for tool-path planning for automated polishing. This work is an integral part of the research program on automated polishing/deburring being carried out at Ryerson University. Whereas tool-path planning for machining is treated as a geometry problem, it is shown here that tool-path planning for polishing should be treated as a contact mechanics problem because of the contact action between the polishing tool and the part surface. To develop this algorithm, contact mechanics is applied for contact area modeling and analysis. Once the contact area is determined, for multiple contact points along the given polishing path, a map of the contact area is generated and utilized to show the coverage area during polishing. This map is then used to plan a polishing path that ensures complete coverage for polishing. Simulation has been carried out to show the effectiveness of this new polishing path algorithm.

Acknowledgements

I would first and foremost like to sincerely thank my supervisor Dr. Jeff Xi for his support and guidance throughout my Graduate Studies. Without his persistence I honestly feel that I would not be where I am today. With his strong theoretical background and understanding of many engineering concepts, he has helped me solve many difficulties whenever I needed help. I was always intrigued by his innovative ideas and solutions to many problems in engineering. He is very devoted to his work and is one of the few professors I know who would go out of his way to help me when needed. It has been my pleasure to work under his supervision.

I also wish to thank my lab mates Dr. Yuwen Li who is working on robotic riveting, Mr. Daniel Finistauri, who is working on reconfigurable robots, and Mr. Haibin Jia

Finally, I would like to sincerely thank my family and close friends for their encouragement, support, and understanding over the course of my university career.

Table of Contents

Author's Declaration ii
Abstract iii
Acknowledgements iv
Table of Contents v
List of Figures vii
Nomenclature ix
1 INTRODUCTION 1
1.1 Background on polishing and tool-path planning 1
1.2 Research objectives and scope 4
1.3 Thesis outline 5
2 LITERATURE REVIEW 6
2.1 Polishing process 6
2.2 Manual polishing 8
2.3 Automated polishing 9
2.4 Polishing tools 11
2.5 Contact mechanics 12
2.6 Path planning 14
2.7 Tool-path distribution 14
2.8 Motion planning 16
2.9 Tool path algorithms 17
2.9.1 Iso-planer 17
2.9.2 Iso-parametric 18
2.9.3 Offset path 19
2.9.4 Iso-scallop 19
2.9.5 Iso-conic 20
2.10 Path planning CNC machines 21
2.11 Path planning for robot polishing 22
3 CONTACT MECHANICS 24
3.1 Model development 24
3.2 Model assumptions 25
3.3 Point contact before loading 26
3.4 Surface contact after loading 27
3.5 Frame of reference 30
4 COVERAGE AREA MAP 31
4.1 Coverage area map (*CAM*) for discontinued raster motion 32
4.2 Coverage area map (*CAM*) for continuous raster motion 35
5 POLISHING PATH: CONSTANT STEPOVER SIZE 38
5.1 Polishing tool 38
5.2 Part with two fixed radii of curvatures 39

5.3 Part with one fixed and one changes radii of curvatures 45
5.4 Part with two changing radii of curvatures 53
6 POLISHING PATH PLANNING 57
6.1 Algorithm for generating polishing path..... 57
7 MODIFIED POLISHING PATH..... 61
7.1 Part with two fixed radii of curvatures 61
7.2 Part with one fixed and one changing radii of curvatures 62
7.3 Part with two changing radii of curvatures 64
8 CONCLUSIONS AND FUTURE WORK..... 68
9 REFERENCES 70
10 APPENDIX A..... 74

List of Figures

Figure 2-1: Bonded abrasives polishing tools 7
Figure 2-2: Manual polishing machines 8
Figure 2-3: Robot polishing process 10
Figure 2-4: a) raster motion b) spiral motion c) discontinued raster motion d) contour path 15
Figure 2-5: Possible end-effector movements 16
Figure 2-6: Iso-parametric curves 18
Figure 2-7: Iso-parametric tool path 18
Figure 2-8: Iso-scallop tool-path 19
Figure 2-9: Iso-conic - tool posture determination 20
Figure 3-1: a) Initial contact point b) Radius of curvature 25
Figure 3-2: Corresponding points 26
Figure 3-3: Contact area 27
Figure 3-4: BA vs. k 29
Figure 3-5: Frame of reference 30
Figure 4-1: Contact area at point *N* 32
Figure 4-2: Discretizing arbitrary part surface 33
Figure 4-3: Coverage area for a discontinued raster path 34
Figure 4-4: Coverage Area Map for a flat surface 36
Figure 5-1: Flat surface plus polishing tool 39
Figure 5-2: Flat surface with continuous raster path 40
Figure 5-3: k vs. tool location 40
Figure 5-4: Semi-major and semi-minor axes vs. tool location 41
Figure 5-5: Stepover size vs. tool location 41
Figure 5-6: Coverage area map for a flat surface 42
Figure 5-7: Flat surface with large stepover size 43
Figure 5-8: Flat surface with small stepover size 44
Figure 5-9: Semi-elliptic tube plus polishing tool - Front view 45
Figure 5-10: Semi-elliptic tube plus polishing tool - Isometric view 46
Figure 5-11: maximum part radius vs. tool location 47
Figure 5-12: *k* value vs. tool location 48
Figure 5-13: major-axis and minor axis vs. tool location 49
Figure 5-14: Coverage area for a single discountinued path 50
Figure 5-15: Large stepover size 51
Figure 5-16: Small stepover size 52
Figure 5-17: Semi-ellipsoid part surface 53
Figure 5-18: Projection of the ellipsoid 54
Figure 5-19: Raster polishing path with fixed stepover size for an ellipsoid 55
Figure 5-20: Polished ellipsoid with raster tool-path 55
Figure 5-21: Crowding and unpolished areas for an ellipsoid 56
Figure 6-1: Coverage area map for modified polishing path 58
Figure 7-1: Modified polishing path for a flat surface 61
Figure 7-2: Modified *CAM* for semi-spherical part surface 62
Figure 7-3: Modified polishing path for semi-spherical part 63

Figure 7-4: Unpolished area on the modified polishing path 63
Figure 7-5: Modified *CAM* for ellipsoid 64
Figure 7-6: Modified polishing path for ellipsoid 65
Figure 7-7: Wire frame design of an ellipsoid 66

Nomenclature

Symbol	Definition
a	Semi-major axis of an ellipse
b	Semi-minor axis of an ellipse
E_1	Young's modulus of elasticity for body #1
E_2	Young's modulus of elasticity for body #2
$K(k')$	Complete elliptic integral of first kind
$E(k')$	Complete elliptic Integral of second kind
k	Ratio of semi-major axis a to semi-minor axis b
R_1	Maximum radius of curvature of body #1
R_1'	Minimum radius of curvature of body #1
R_2	Maximum radius of curvature of body #2
R_2'	Minimum radius of curvature of body #2
N	Single contact point
CA	Contact area

Greek Symbols

υ_1	Poisson ratio of body #1
υ_2	Poisson ratio of body #2
$\emptyset$	Intersection angle between planes generated between R_1 and R_2
$\forall$	For any
$\exists$	There exist
$\mid$	Such that
$\Rightarrow$	Implies that

1 INTRODUCTION

This chapter provides an introduction to the polishing process and highlights the reasons for automating it. The chapter continues with brief introduction to tool-path planning and identifies problems associated with traditional approaches in the field. Subsequently, the research objectives are presented along with the thesis outline.

1.1 Background on polishing and tool-path planning

Design of aircrafts, satellites and other defense systems involves manufacturing of engineered components with complicated geometries. These components have design specifications and tolerances down to a few microns. Maintaining these specifications is an important factor in the aerospace industry for several reasons:

1) Maintaining aerodynamics properties.
2) Eliminating crack initiation and propagation processes.
3) Reducing stress concentration points.
4) Allowing proper fit between components.

For these reasons polishing process is utilized subsequent to traditional material removal processes (i.e. cutting, machining or grinding) [1]. Research on grinding and polishing processes has been conducted by Malkin [2] where he claims that most precision components have been either machined by grinding or polishing at some stage of their production or processed by machines which owe their precision to abrasive operations.

Polishing is an abrasive operation that improves the surface quality through the removal of scratches, machining marks, pits, and burrs including smoothing rough surfaces by means of micro abrasive grains [3]. The process involves material removal by the rubbing action between the part surface and the polishing tool. Polishing is one of the final stages employed in manufacturing to remove unwanted material and to introduce desired surface quality. The

polishing process indicates that excess material has been previously removed from the part and the only operation that still remains is to bring the part to the desired design specifications.

The high levels of process automation and control in manufacturing environments today are not reflected on polishing process where highly skilled workers are spending enormous time and resources on manual or semi-automated polishing processes. As a result, there are negative consequences for this, as follows:

1) Manual polishing involves a high risk of injuries as a result of the interaction between operator and moving machinery. Therefore, in recent years, the aerospace industry has been pushing towards safer environments for their employees, and many resources have been allocated to reduce operator / moving machines interaction [4].

2) Manual polishing consumes gross amounts of resources and time as it is a manual operation in nature. Ahn, Lee, and Jeong [5] have studied automated polishing for the tool and die industry. They reported that the polishing process is labor intensive and time consuming, occupying up to 30–50% of the entire die manufacturing time. On the same note, Guvenc and Srinivasan reported that a traditional polishing method in the mold making industry consumes 37% of manufacturing time [6].

3) Manual polishing heavily relies on skilled labor where the operator uses his experience and judgment to bring the part surface to an excellent surface roughness [7]. This skilled labor is vanishing from the manufacturing industry and the younger generation does not want to be trained in this special trade and prefers to resort to automation and robotics.

For these reasons, the aerospace industry and research institutions worldwide are putting a lot of emphasis on robotic polishing systems. According to Lambie [4], automating the polishing process would be invaluable in the aerospace industry and bring substantial cost savings.

Polishing path planning is one aspect of interest in robotic polishing systems. Polishing path planning attracts experts from various fields including engineers, mathematicians and computer scientists. Extensive research has been done in the field and many approaches have been

developed for various machines including numerical control (NC) and industrial robots. Dragomatz classified the studies for tool-path planning of NC milling. He reports an enormous number of studies that have been done in the field [8]; however, not enough research has been done on tool-path planning for robotic polishing.

In general, robotic polishing path denotes the locus of points in the operational space that a manipulator has to follow in the execution of the assigned motion. Thus, the polishing path is a pure geometric description of motion [9]. The polishing path is defined as a series of straight lines, arcs and connecting bridges that dictates the tool motion along the part surface. The lines and arcs are collections of discretized points along the part surface and are known as "cutter locations". The cutter location data are generated with the assistance of commercially available CAD/CAM packages. Once cutter location data have been determined, the executable production codes are generated [10]. Thus, any surface is approximated by a series of straight lines and arcs for polishing.

Conventional polishing path strategies do not take into consideration the coverage area generated between the polishing tool and the part surface as a result of the contact action between the two. Generally, polishing paths are designed with fixed stepover size between two adjacent paths. However, there are problems associated with fixed stepover size and they are as follows:

1) Large stepover size: an envelope of unpolished region is generated between the paths. This envelope indicates that the polishing tool did not come in contact with the part at this region and it results in a rough surface. In this case, additional paths are required as to remove the rough surface and guarantee full coverage during polishing.

2) Small stepover size: results in overlapping between adjacent paths. Overlapping may degrade the part surface and decrease polishing tool life as the same area is covered more than once. This results in increased production time and manufacturing costs.

In addition, the part surface does not necessarily have to be flat but could have varying slopes and curvatures which results in a complicated coverage area map. The research conducted herein shows a 2-D coverage area map that highlights the problems associated with fixed stepover size.

Once these problems are identified, a novel approach for polishing path planning is proposed. The approach for polishing path is based on the contact area generated between the polishing tool and the part surface under applied compressive force. The approach is tested for three scenarios:

1) 2 fixed radii of curvatures (i.e. flat surfaces)
2) 1 fixed radius of curvature + 1 varies along the part surface (i.e. semi-spherical tube)
3) 2 varying radii of curvatures (i.e. ellipsoid)

Full coverage area is obtained for the first two cases and the number of polishing path is reduced. However, an approximation method had to be implemented for the third case and subsequent research is required.

1.2 Research objectives and scope

This work is an integral part of a continuous research program on automated polishing and deburring being carried out at Ryerson University. The research is funded by the Consortium for Research and Innovation in Aerospace in Quebec (CRAIQ) under MANU-409 project on automated deburring and part finishing [11]. Whereas tool-path planning for machining is treated solely as a geometry problem, it is shown here that polishing tool-path planning should be treated as a contact mechanics problem. The objectives of this work are as follows:

1. Modeling the polishing tool and part surface interaction using Hertzian contact theory.
2. Applying the model to consecutive contact points along the part surface.
3. Generating the Coverage Area Map *(CAM*) which is a 2-D map that shows the contact area between the polishing tool and the part surface for consecutive points.
4. Developing a polishing path algorithm using the Coverage Area Map (*CAM*).
5. Simulating and testing the algorithm for various part surfaces.

1.3 Thesis outline

The thesis consists of 7 chapters and is organized as follows:

In Chapter 2 key publications that have contributed to the research field of polishing path planning are presented. In addition, the chapter provides an overview of literature and scholarly works pertaining to the research and development of the theory presented herein.

In Chapter 3 Hertzian contact theory is presented. The chapter introduces the theory of contact area generated between two separate objects under constant compressive force at a single contact point. The theory presented herein is crucial for understanding the rest of the thesis.

In Chapter 4 the novel contribution of the thesis is presented. The chapter introduces the coverage area during robotic polishing which results in the development of Coverage Area Map (*CAM*).

In Chapter 5 the Coverage Area Map (*CAM*) is applied to polishing path with constant stepover size. Two major problems with constant stepover size are identified and discussed.

In Chapter 6 an algorithm for modified polishing path based on the Coverage Area MAP (*CAM*) is developed. The algorithm ensures complete coverage of the surface during robotic polishing.

In Chapter 7 the modified polishing path algorithm is tested for various part surfaces. The results show that the drawbacks of conventional raster method are eliminated.

Finally, the thesis is completed by the conclusions presented in Chapter 8. The chapter includes a discussion about the method and its effectiveness. The chapter also highlights the main contributions of this research and presents recommendations for future studies. Followed by this chapter comes the Reference section and Appendix section respectively.

2 LITERATURE REVIEW

The following chapter provides a detailed literature review and lists key publications that have contributed to the development of existing robotic polishing processes. The chapter continues with detailed descriptions of conventional tool-path strategies and examines existing efforts, both past and current, in continuously improving the tool-path.

2.1 Polishing process

The polishing process is a finishing operation that indicates that the part surface has had all the excess material removed and the only operation remaining is to bring the part to the required surface finish. In general, the polishing process involves material removal by the rubbing action between the polishing tool and the part. The process is mainly used to remove scratches, machining marks, pits, and burrs and to smooth rough surfaces by means of abrasive grains [12]. A good deal of the process is for surface improvement for the sake of its appearance, and deburring for better operation of the part. The material removal in the polishing process is achieved by abrasives materials. Abrasives are micro cutting tools made of small bits of grains of hard mineral. In grinding and polishing applications these grains are used either in bonded or loose forms. When the grains are bonded they are shaped into wheels and discs of many shapes and sizes. In the bonded form, the abrasive grains act like a milling cutter or turning tool, with perhaps thousands of cutting teeth instead of the dozen or so characteristic on a typical milling cutter.

Several methods have been developed for the polishing process; however, researches mainly focused on two polishing processes, namely, loose and bonded. The former is usually used for fine polishing, where an abrasive media is supplied to the gap between a non-abrasive tool and a part. The latter is normally used for general polishing, where a bonded abrasive tool is directly pressed against a part. Bonded abrasives include stones, disks, wheels, belts canvas and felt. Figure 2-1 shows various polishing tools.

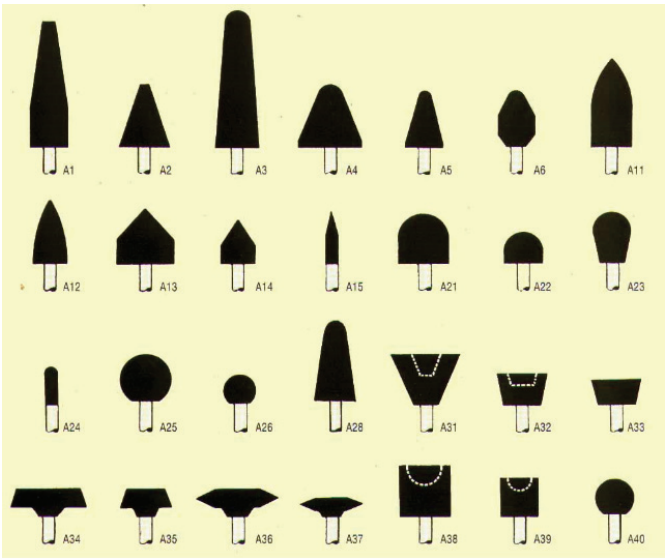

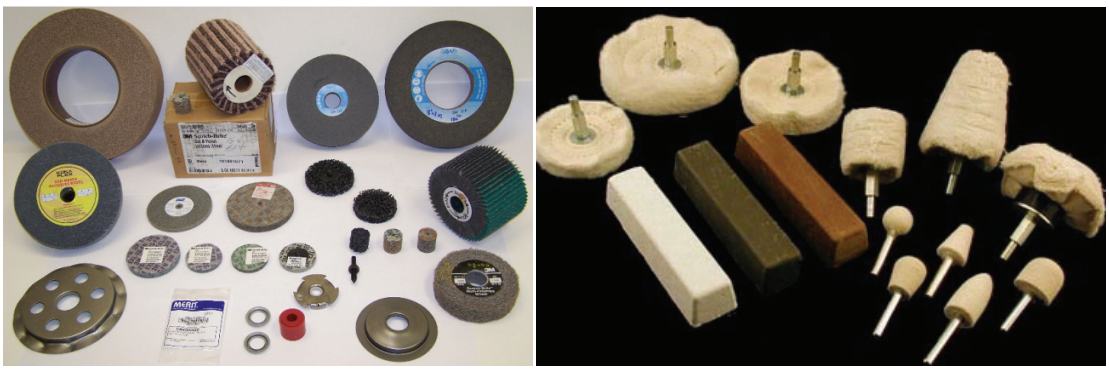

Figure 2-1: Bonded abrasives polishing tools

The cutting conditions in polishing are characterized by very high speeds and very small cut size, compared to traditional machining operations. The polishing wheels are generally rotating at a speed of 2300 m/min (7500 ft/min). The wheels are made of canvas, leather, felt, or even paper; thus the wheels are somewhat flexible. The abrasive grains are glued to the outside periphery of the wheel. After the abrasive have been worn down or used up, the wheel is replenished with new grits. Grit sizes of 20-80 are used for rough polishing, 90-120 for finishing polishing [12].

Most commercial polishing is performed to achieve a surface finish that is superior to that which can be accomplished with conventional machining or grinding. The surface finish of the part is affected by the size of individual chips formed during polishing. Surface roughness for polishing is about 0.025-0.8 μm (1-32μ-in) as compared to other abrasive processes such as grinding with fine grit size 0.2-0.4 μm (8-16μ-in) [12].

2.2 Manual polishing

The polishing process has been done manually by highly skilled operators with specialized polishing tools. In general, the parts are taken from the machines and polished using hand tools and grinders. This type of polishing is time consuming and error prone. For precision products, specifications for roughness and surface integrity can be rather stringent and manual polishing may not be feasible. Polishing is performed using either the periphery of the polishing tool or the flat face of it. Since the work is normally held in a horizontal orientation, peripheral polishing is performed by rotating the polishing tool about a vertical axis. In either case, the relative motion of the part is achieved by reciprocating the work past the wheel or by rotating it.

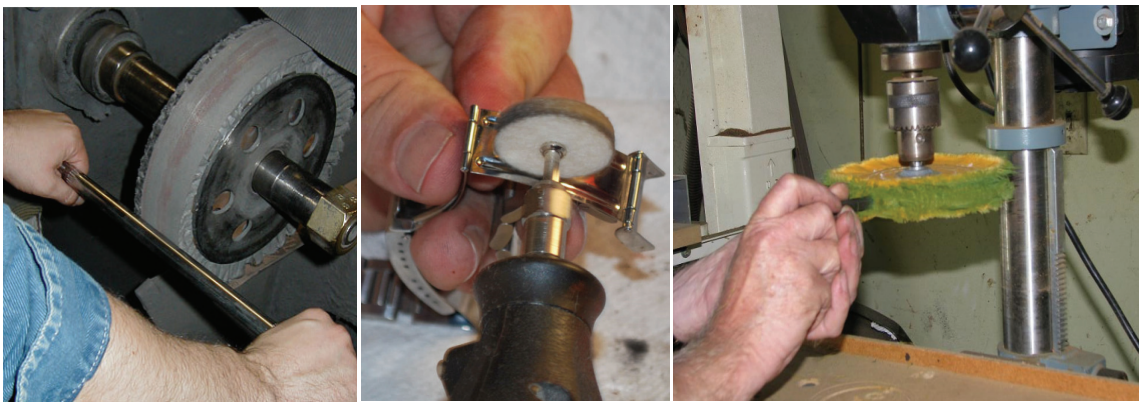

Figure 2-2: Manual polishing machines

Figure 2-2 shows various polishing machines used in industry for manual polishing process.

4) Manual polishing involves a high risk of injuries as a result of the interaction between operator and moving machinery.
5) Manual polishing consumes gross amounts of resources and time as it is a manual operation in nature.
6) Manual polishing heavily relies on skilled labor where the operator uses his experience and judgment to bring the part surface to an excellent surface roughness.

For these reasons, a lot of emphasis is being put on robotic and automated polishing systems. No doubt, automating the process would be invaluable in the aerospace industry and bring substantial cost savings.

2.3 Automated polishing

The current industrial environment demands shorter manufacturing cycles as the pressure on manufacturing prices has significantly increased. This in turn threatens the aerospace industry since the geometry of aerospace parts has drastically increased and so the manufacturing time. Polishing is an expensive, time consuming, labor intensive, and error prone. Mistakes committed by a human operator at this stage may result in expensive re-working or even scrapping of the manufactured parts. In order to increase cost efficiency and to reduce exposure to human errors it is very desirable to automate surface polishing by machines. As an attempt to reduce manufacturing cycles, automated polishing has been the subject of much experimentation and research, particularly in North America. Existing polishing processes have become more sophisticated and demands exceptional skill of an experienced master. It would be difficult to increase productivity if the manual polishing processes are not automated. Therefore, the manufacturing industry, aerospace in particular, are continuously pushing towards automating the polishing process. Automating the polishing process has been widely studied during the last decade. Several new methods have been proposed recently.

In general, there are two types of candidate machine for automated polishing:

1. Machine tools: structurally more rigid and are suitable for tasks that require higher accuracy or larger processing force.
2. Industrial robots: dexterous but the payload is smaller and capable of positioning and orienting end-effector tooling according to the shape and contour of part surfaces;

Although it is necessary to maintain a steady tool part-surface contact, polishing does not require processing force as large as those in machining operations. Polishing also does not require as high a positioning accuracy. Thus, industrial robots are potentially more suitable for surface polishing automation than machine tools.

Guvenc [6] has studies robotic polishing for the die and mold industry where he claims that approximately 37% of manufacturing time is allocated to finishing of the mould cavity's surface. According to [13], the large percentage of time indicates the complexity of the tool motions

necessary, the wide variety of tooling utilized, as well as measuring and recording the surface quality during the process. Figure 2-3 shows an industrial robot polishing process where the polishing tool is held fix while the part is attached to the end-effector. In this case, large industrial robot is required capable of carrying large payload to provide the relative motion between the polishing tool and the part surface. Another method is to fix part and attach the polishing tool to the end-effector. In this case, smaller robots are utilized as the payload is much smaller; however, robot excitation results from the rotating motion of the polishing tool.

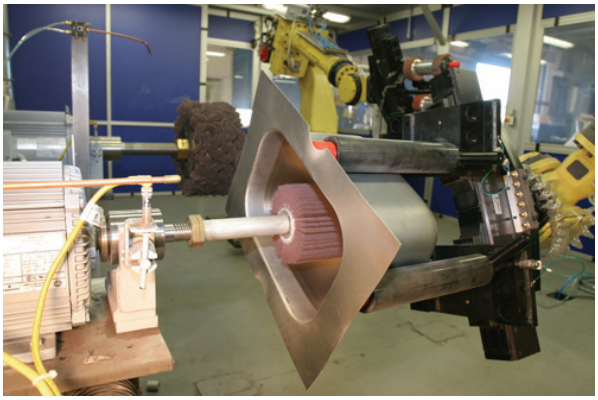

Figure 2-3: Robot polishing process

Robot polishing is affected by two main factors as identified by Tsai, Huang, and Kao. First, kinematics parameters which are controlled by the polishing robot and include feed rate of the polishing tool, rotational speed of the tool, polishing path, polishing pressure, etc. The other factors that affect polishing results come from the physical properties and type of the polishing tool and part. These factors can be grouped according to the material hardness, initial surface roughness, tool type, and the abrasive material and its grain size [14].

Polishing parameters include the polishing normal force, the spindle speed and the feed rate. Within each cycle, the tool follows a continuous path to sweep through the part surface under fixed polishing parameters. In his research of polishing process with special machine tools, Wang [15] claims that force and position control of robot polishing can be finished steadily. However, it is difficult for finishing of free-form surfaces since that the trajectory error is relatively great. Due to the diversification and irregularity of mould surfaces, polishing tools must change movement trajectory with surface shape of workpiece in process.

2.4 Polishing tools

For many years the obstacle to automatic control of polishing operation was the unpredictable wear of the cutting tool resulting in out-of-tolerance part surfaces. But new developments in polishing tools have made cutting tools much more predictable. The cutting tool for conventional machining is often called “hard tool” as it held rigid during machining. Hard tools are not flexible and cannot change to fit the geometry of a given work-piece, nor it can adjust to shape or force changes should it encounter any [13]. The polishing tool, on the other hand, is often called “soft tool” as it held with compliance, either passive or active. The mentioned compliance affects the polishing area and therefore it must be determined using contact mechanics. Most of the existing robotic and CNC processes use non-complaint tooling, briefly this means that these tools cannot adjust to sudden irregularities in the surface geometry or to wear.

With the realization of the benefit of switching to automated polishing technique many researches choose to investigate the development of compliant polishing tools. Compliance is a trait that the end effector has the ability to compensate or comply in a particular axis when a contact force or positional error is presented; in other words it is a means to accomplish force or position control [13]. While robots can meet the flexibility requirement for polishing systems, the positional accuracy of existing industrial robots is generally poor. A common solution to the problem involves the addition of compliant elements between the robot and the polishing tool. Considerable work has been done using compliant polishing end-effectors. In general compliance tools feature compliance in two orthogonal directions in the form of replaceable springs and fluid dampers. In the study of polishing and deburring systems Liao [16] claimed that the deburring process of manufactured parts has been investigated theoretically and experimentally as a frequency domain control problem with special regard to application by industrial robot manipulators. Liao developed a new control strategy for precision deburring that guarantees the burr removal while compensating for robot osculation and small uncertainties in the location of the part relative to the robot. The compliant tool-hold designed according to the above control strategy provided the required normal and tangential forces for deburring. Tsai [7] presented an automatic mould polishing system consisting of a five-axis robot and a force-

control mechanism and developed and efficient automatic polishing process with a new compliant abrasive tool.

Researchers have generally broken the study of compliance down into two main categories of study: active compliance and passive compliance. An active compliance rotary end-effector was developed by Mizugaki [17], with the objective of preventing over-polishing around a corner edge of a part surface. By adjusting the length of a compression spring, the system was sensitive enough to adjust the polishing force and accommodate minute changes of the part surface as the polishing tool approached an edge of a part surface. There have been attempts to use passive devices to reduce changes of the contact force during polishing caused by small positioning and orienting errors of the polishing robot. Takeuchi [18] developed a polishing tool that regulated the contact force by a mounting interface of a linear roller slide and an air piston. In addition, Furukawa [19] developed an automatic polishing system that uses passively compliant end-effector mounted on the wrist of an industrial robot. This system was used for polishing an unknown three-dimensional surface.

2.5 Contact mechanics

Understanding of the contact problem during polishing, resulting from the interaction between the polishing tool part surfaces, is crucial to ensure a complete polishing coverage using conventional tool-path algorithms. When a set of raster paths is used, small stepover size could lead to low polishing efficiency as a large number of tool passes is required and while large stepover size results in large percentage of unpolished area between two adjacent passes. In light of contact mechanics, the coverage area is not only related to the diameter of the tool but also related to geometric characteristics (radius of curvature) of the part surface. For free form parts with complex geometries there is no analytical way of determining the coverage area and the corresponding step-over size.

Though the constant contact stress theory has been recently proposed to develop the proper control strategy for controlling the polishing force between the tool and part surface [16], [20],

and [21], the current practices in industry still rely on constant force during polishing. For polishing with abrasives, a steady contact area between the tool and the part surface throughout a polishing cycle is critical to obtain good surface finishing. However, the contact area between the polishing tool and the part surface keep changing with the radii of curvatures. This results in varying coverage area along the tool path. Therefore, polishing tool-path algorithm must resort to contact mechanics theory to generate polishing path that guarantees full coverage area along the part surface.

In general, contact area is the area generated between two non-conforming objects under applied compressive force. The contact area is the range of contact between the polishing tool and the part surface in a specified direction. According to the Hertzian contact theory, the contact area is elliptic in shape and depends on the principal radii of curvatures at the contact point and the magnitude of the applied compressive force between the two objects. An elaborated discussion of the Hertzian contact theory is provided in chapters to follow. In the mean time, it is important to understand that under constant pressure the contact

In the attempt to automate the polishing process, Tsai, Huang, and Kao developed the uniform material removal (UMR) model for an automatic mold polishing system (AMPS). They recognized that the contact area between the polishing tool and the part varies from point to point on a free-form surface. Therefore, they tried to ensure constant contact pressure during polishing over the entire mold surface and they assumed that the polishing normal force distributes evenly on the effective contact area to produce the desired constant pressure [14].

An important part of robotic surface polishing is tool-path generation. Whilst a basic requirement for polishing tool paths is that the surface can be completely covered during a polishing cycle, for time and quality considerations an important criterion in determining the polishing tool path is how evenly the part surface is covered. Even covering suggests that the unit area of the surface at each location receives a similar amount of polishing. For time efficiency considerations, even coverage implies the shortest cycle time. The next section introduces the various tool-path distribution methods and tool-path algorithms.

2.6 Path planning

Tool-path planning is an attractive research area and gets the attention of experts from many fields including mechanical and electrical engineers, computer scientists and mathematician. A large amount of research related to tool-path planning has appeared in literature. However, the use of that knowledge is difficult for three main reasons [22]:

1. Finding relevant research papers: enormous amount of papers have been published in many areas of tool-path by many researches and experts in the field. When searching for research papers one can easily get lost between hundreds of papers.
2. Subject specific research: many researches and experts in various fields address the problem of tool-path planning. A research paper related to tool-path planning may focus on a specific issue from one of these fields (i.e. mechanical engineering, computer science etc.) and have no relevance to other fields.
3. Subject specific terminology: tool-path planning has been studied by specialists from various fields using subject-specific and unfamiliar terminology.

For these reasons the use of knowledge presented in various research papers in the field become cumbersome. The following section presents conventional and generally accepted strategies for tool-path planning among new research and other aspects of tool-path.

2.7 Tool-path distribution

Many tool-paths distribution strategies have been developed; they are classified into four main categories, namely, continuous raster path, offset path, discontinuous raster path and contour path [23] [24].

1. Continuous raster paths: the polishing tool moves back and forth across the part surface with constant stepover size between paths, see Figure 2-4 (a). This strategy also found in literature as zigzag, staircase or sweep tool-paths.
2. Offset paths: the polishing tool starts at the outer edge of the part and proceeds inwards towards the center of the part in spiral motion (or vice versa) see Figure 2-4 (b). For

every revolution of the tool around the part surface the distance from the center changes. This strategy is also found in literature as spiral polishing paths.

3. Discontinuous raster paths: the polishing tool moves in parallel direction for every pass along the part surface. The tool then, retracts from the part surface and moves back to the starting point across adjacent path. This process continued until the entire part surface is completely covered; see Figure 2-4 (c).
4. Contour path: the polishing path is executed by a three steps process. First, for every contour element, an elementary offset element is constructed. Second, gaps between the offset elements are closed by joining arcs—this results in some closed path. Third, self-intersections of the curves are eliminated and portions of the curves are cleared away yielding the final offset curves; see Figure 2-4 (d)

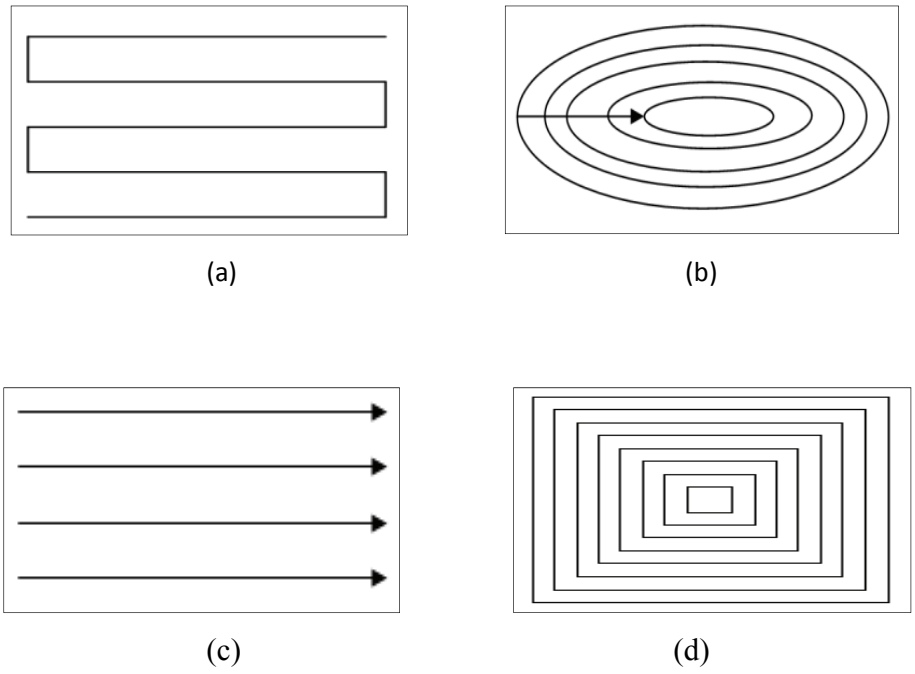

Figure 2-4: a) raster motion b) spiral motion c) discontinued raster motion d) contour path

2.8 Motion planning

Tool-path consists of a set multiple contact points along the part surface. The end-effector follows these points and generates a continuous path that covers the entire surface. According to Yao [25], three types of end-effector movements are possible as shown in Figure 2-5:

1. Effective move: the end-effector moves along the path that has not been covered yet.
2. Repositioning: the end-effector moves in the region that has been fully covered before.
3. Retraction: the end-effector disengaged from the part surface to a clearance height and moved to another position using rapid movement where it is lowered down to perform another cycle.

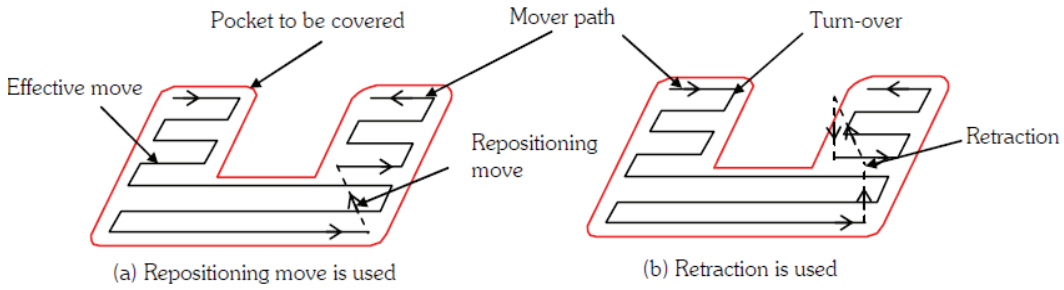

Figure 2-5: Possible end-effector movements [25]

The end-effector movements are generated as an input to the motion control systems which ensure that the manipulator executes the planned trajectories. For clarification throughout this thesis, a path is defined as the locus of points in the joint space (operational space) that the manipulator has to follow in the execution of assigned motion. Thus, a path is then a pure geometric description of motion, and trajectory is defined as a path on which time laws are specified (*i.e.* velocities and accelerations). There are two main trajectory generation methods for the execution of a defined tool-path:

1. Point-to-point motion: where the manipulator moves from an initial to a final joint configuration in a given time. In this case the path is of no concern. This method is also called positioning system.
2. Continuous path: where sequence of points are assigned as to guarantee better control of the executed path.

Stepover size refers to the distance between two adjacent paths that the end-effector has to follow in the execution of path along the part surface. The stepover size is determined by the diameter of the polishing tool and given as a percentage (stepover ratio) of the tool diameter [26]. However, this determination method is based on the principle of conventional machining, and does not represent the coverage area between the polishing tool and the part surface. Whereas tool-path planning for machining is treated as a geometry problem, it is shown here that polishing path should be treated as a contact mechanics problem as a result of contact action between the polishing tool and the part surface. There are various algorithms for calculating the stepover size and tool-path as discussed in the next section.

2.9 Tool path algorithms

In general, tool-path algorithms are classifies into five main groups: the Iso-planar, Iso-parametric, offset path, the Iso-scallop and the Iso-conic. A new algorithm has been proposed now which is the Iso-conic tool-path. The determination of the contact paths has universally been in the offset fashion. An initial contact path is first decided (base path) and subsequent paths are just offset paths of the previous one with a constant stepover size measured in the parametric domain on the part surface.

2.9.1 Iso-planer

The Iso-planar algorithm is one of the earliest methods for generating tool-paths. In the Iso-planer algorithm, the tool follows planar cross-sections generated by intersecting used specified surfaces with a set of parallel planes. This approach is also referred to as Cartesian tool-path planning. In this algorithm, instead of parametric increments, the distance in u and v directions must be obtained in order to move the slicing plane across the surface. The path interval or the distance between the vertical planes is determined based on the scallop-height limitation [27]. Generating tool paths along planar intersection curves is a very common method and improved planar section tool path generation methods that take into consideration maximum inaccuracy of the manufactured part have been developed. The disadvantages of using this algorithm of using plane sections as tool path are (a) large tool path length and, (b) part geometry is neglected [28].

2.9.2 Iso-parametric

Iso-parametric paths generation requires determination of the smallest tool path interval at each adjacent path. The tool path interval is used as a constant offset in the next tool path [29]. The reason for selecting the smallest interval as the offset distance is that it makes it easy to define constant Iso-parametric offset as the next tool path that satisfy surface accuracy. The algorithm is the inefficient resulting in non-predictable scallop remaining on the part surface. In addition, adjacent tool-path is generated by the smallest path interval between two paths implies that redundant machining overlap occurs between the paths. The algorithm traces guiding cutters along constant parametric curves on the part surface as seen in Figure 2-6. The distance between parallel trajectories is the parallel CC path interval. The Iso-parametric tool-path also referred to as parametric machining [30].

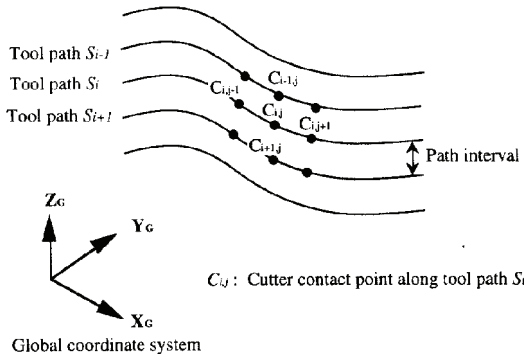

Figure 2-6: Iso-parametric curves

Except for a few particular part surfaces, the generation of continuous Iso-parametric tool paths for compound surfaces is generally not possible. The Iso-parametric tool paths are much denser in one surface than others due to the non-uniform transformation between parametric and Euclidean spaces [31], resulting in varying scallop height distribution and non-optimal machining time [32]. Figure 2-7 shows the Iso-parametric path on an arbitrary part surface [33]:

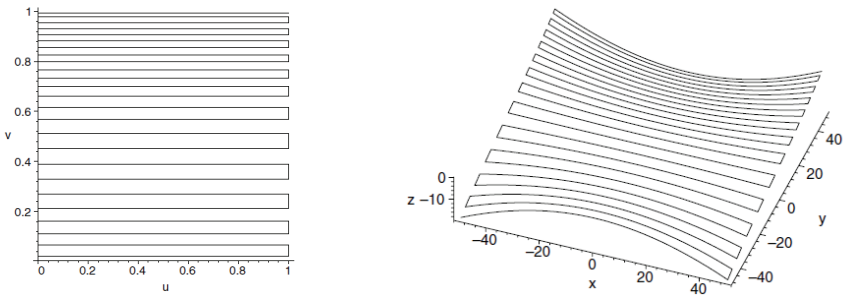

Figure 2-7: Iso-parametric tool path

2.9.3 Offset path

Offset tool-paths play a crucial role in path generation for NC machining and robot path planning. Offsets paths are rather complex geometrical entities and finding offset paths is a global problem, because a global minimum of the distance is sought [34]. Offset paths received considerable attention since they describe the displaced path that tool center must execute to cut a prescribed path [35]. Offset paths offers desired accuracy on the manufactured part. Of all the tool-paths algorithms available, this gives the potential of offering the user a direct control over the accuracy of the manufactured part [28].

2.9.4 Iso-scallop

Recall that, in the Iso-parametric algorithm the tool is driven along parallel planes. In this algorithm, only the maximum scallop height between two adjacent paths can be controlled [36]. In order to control the scallop height on a specific area the entire tool path has to be tightened. This strategy ensures constant scallop height throughout the part surface. Therefore, it is named iso-scallop algorithm. When the scallop height remains constant throughout the tool-path, scallop curve are design to lay on surface of the scallop height. Starting from the base path, an intersection curve of the swept volume with constant scallop height surface is computed. Based on the computed curve an adjacent path is found.

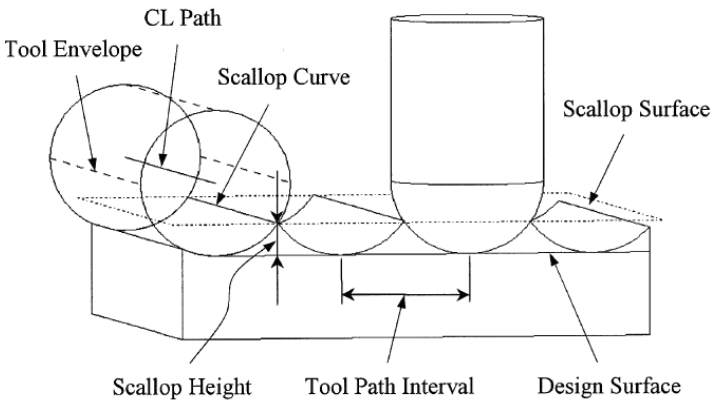

Figure 2-8: Iso-scallop tool-path

2.9.5 Iso-conic

In the study of tool-path generation, Wang [37] presented the iso-conic strategy for 5-axis tool-path algorithm that aims at alleviating problems associated with traditional tool path algorithms. Conventional tool-path algorithms treat the tool-path placement as a decoupled problem and treat the CC curve placement independently from tool orientations. This incurs many undesired problems as described by Wang:

1. Abrupt change of tool orientations
2. Reduced efficiency in machining
3. Reduced finishing surface quality
4. Unnecessary dynamic loading on the machine

In his study, the cutter contact curves are contour lines on the part surface that satisfy the iso-conic property – the surface vectors on each cutter contact curve fall on a right small circle on the Gaussian sphere and the tool orientation associated to a cutter contact curve are determined by the principal of minimum tilt angle that seeks fastest cutting rate without local gouging. The iso-conic algorithm seeks better correlation between cutter contact points and tool orientations and also the overall planning and ordering of the cutter contact curves on the part surface.

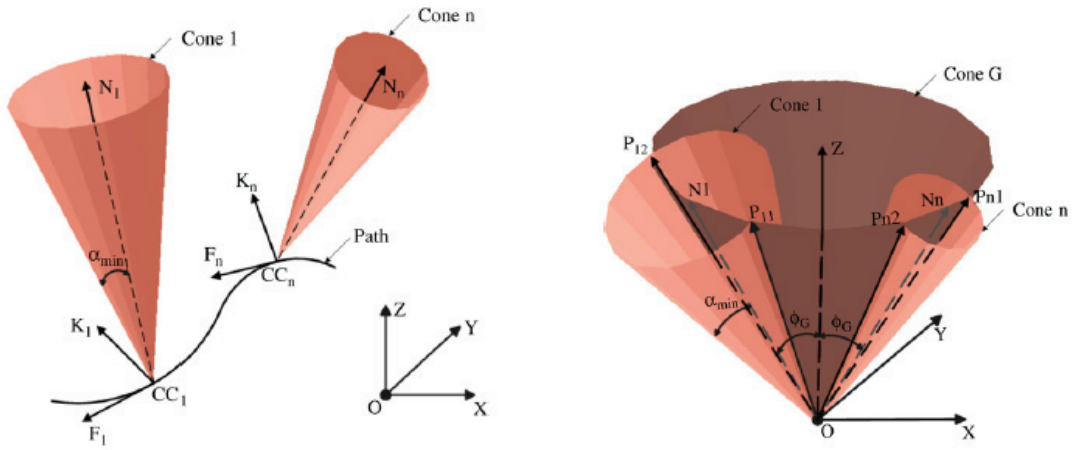

Figure 2-9: Iso-conic - tool posture determination

Figure 2-9 illustrates the tool posture determination method. The key to this method is that the surface normal vectors at the N^{th} CC points CCi, satisfy the iso-conic condition, that is, they all fall on a cone with its apex at the origin.

2.10 Path planning CNC machines

Generating polishing paths for 5-axis CNC machines requires determination of cutter location (CL) points along the part surface. This is a complicated problem since that the tool orientation at each point and polishing parameters (i.e. spindle speeds, traveling velocity etc.) have to be considered individually. It is difficult to solve the problem considering all relevant aspects of generating the path (i.e. pattern, length, parameters, tool orientation, scheduling of the feed rates etc.) [38]. Therefore, many researchers attempted to solve each problem separately. In practice, 5-axis machining suffers from a number of drawbacks, most of which are related to complex tool movement, gouging and tool interference. Because of the two additional degrees of freedom compared to 3-axis machining, 5-axis machining has brought advantages as well as new problems, such as, highly complex algorithms for gauging avoidance and collision detection between the tool and the non-machined portion of the part surface. Most 5-axis tool path generation algorithms take a decoupled two stage strategy: first, the so called cutter contact (CC) curves are places on the part surface; then, for each CC curve, tool orientation are decided that will accommodate local and global constraints i.e. global gouging and global collision avoidance [37]. For the former stage, usually simplistic "offset" methods are adopted to determine the CC curves

Generating polishing paths for milling operation requires determination of part surface at cutter contact point (CC_i) that moves to next point CC_{i+1} linearly. Curved paths are approximated by straight line segment. As a result of linearity approximation, an un-machined region between adjacent tool-paths called scallop or cusp is generated. After machining, a polishing process is required to remove the scallop and bring the part to the required specifications. The polishing process is expensive and time consuming. Therefore, appropriate tool-path in the finish stage is required to reduce the amount of secondary processes. In the research of Non-Iso-parametric tool path, Lee [39] used machining strip evaluation to determine efficient tool-path. In Lee's algorithm, a non-Iso-parametric (varying interval) tool paths are found by calculating orthogonal path intervals using machining strip width evaluation method. The advantage of the approach is that the new path is chosen to be the next path and guarantees no redundant tool motion.

2.11 Path planning for robot polishing

Robotic polishing has many advantages over conventional CNC polishing machines. The advantages arise from the robot flexibility, end-effector compliance, and the capacity to integrate with peripherals. The polishing process does not require large processing forces as those in machining operations and does not require high positioning accuracy. In general, it is necessary to control the axis of the polishing tool in the direction normal to the part surface or at a certain angle from the normal direction and maintain a steady tool part surface contact.

The time duration of the polishing process depends primarily on:

1. Physical dimensions of the polishing tool.
2. Geometry of the part surface.
3. Algorithm of the polishing path selected for the job.

For simplicity, polishing paths are defined as assembly of multiple tool paths along the part surface where each path of the tool across the part surface is known as a single path or discontinued path. To reduce time duration of the polishing process and improve surface quality, it is of outmost importance to prevent, as much as possible, the overlaps between two consecutive tool passes while generating a path that guarantees full coverage of the part surface.

In the study of robotic polishing Tam [40] presented his work of polishing path generation for loose abrasive robotic polishing process. The main focus of Tam's work was on generating polishing path that guarantees evenness along the part surface. Even coverage implies that surface roughness is reduced without introducing surface waviness. Tam claims that in a typical polishing task, maintaining the polishing conditions constant results in material removal that is proportional to the polishing time. This implies that uneven polishing time along the part surface indicates of uneven material removal resulting in undesirable surface waviness. For the study, Tam used scanning polishing paths for enhancing the evenness of free-form surfaces.

When it comes to tool-path planning, none of the mentioned approaches considers the interaction between the part and the polishing tool and the geometric data (i.e. radius of curvature) as a factor that influence the process data (i.e. applied pressure or force) as in the case of automated

polishing. Needless to say that the radius of curvatures of the part and the polishing tool including the applied force are crucial factors that affect the surface contact area during the automated polishing process.

In what follows, first, the contact problem for polishing is described and modeled; the equations for the determination of the contact area are formulated based on work carried out by Roswell [13]. Second, simulation is carried out to obtain a Coverage Area Map (*CAM*) of the contact area for a curved part along a polishing path. Third, discussions are provided as to how to use this map to design a proper path so that the required polishing area can be fully covered.

3 CONTACT MECHANICS

Solving engineering problems requires an analytical equation to be solved from the physical model in hand. In the following chapter, the contact area generated between the polishing tool and the part surface is modeled based on the work carried out by Roswell [13]. An analytical equation is developed using the Hertzian contact theory. The model is important in subsequent chapters when the coverage area map is developed for continuous paths for robotic polishing. The model herein is developed for two separate objects in contact at a single point under applied compressive force. In subsequent chapters, the model is applied for consecutive contact points along the part surface as a basis for guaranteeing full coverage area.

3.1 Model development

A model for the contact area generated between the polishing tool and the part surface is developed in this section. The model is based on Hertzian contact theory as developed in the branch of contact mechanics. Contact area refers to the area generated between two separate non-conforming bodies made of elastic materials under applied compressive force P. Non-conforming means that both bodies have different profiles and the contact area between them is small relative to the dimensions of the bodies themselves [41]. When two non-conforming bodies are coming in contact, with negligible compressive force, they will first touch at a single point. No compressive force is applied at this time. Thus, initially the bodies do not deform as seen in Figure 3-1. For simplicity, the upper body is denoted by B_1 and the lower body by B_2. The first point where the surfaces of B_1 and B_2 interact is referred to the *initial contact point*. If the bodies are assumed to be discs than each disc has a maximum and minimum radii of curvature represented by R_1 and R_1' for the upper disc at the point of contact and R_2 and R_2' for the lower disc. The angle $\emptyset$ is the intersection angle between planes generated between R_1 and R_2.

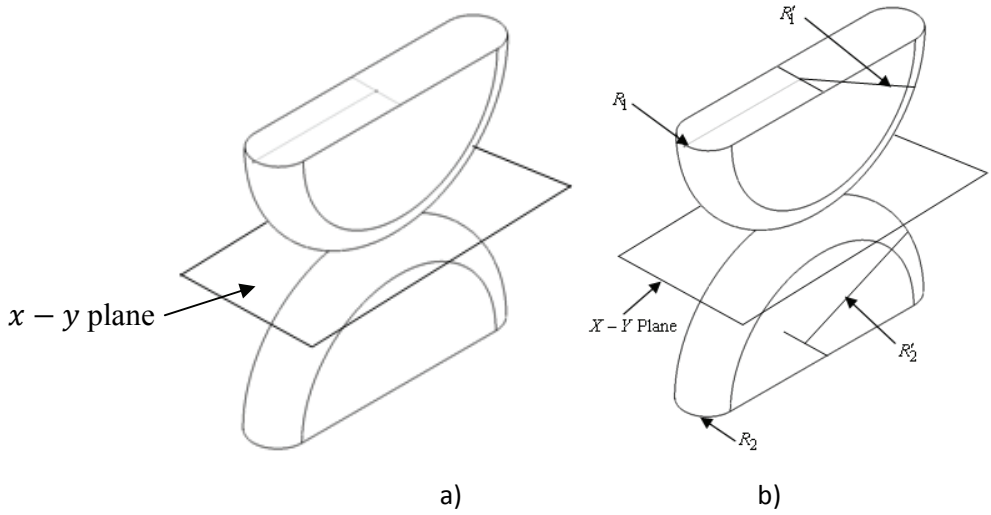

Figure 3-1: a) Initial contact point b) Radius of curvature

3.2 Model assumptions

For the Hertzian contact theory to be applied [42]:

1. The bodies must be homogeneous, isotropic, obey Hooke's law and experience small strains and rotations, (i.e. the linear theory of elasticity applies).
2. The dimensions of the deformed contact area remain small compared to the principal radius of the undeformed surfaces.
3. The contact surfaces are continuous prior to deformation.

In addition, the line of action of the compressive force P is assumed to lay normal to the $x - y$ plane. The compressive force passes through the point of contact and through the centers of curvature of both discs. Therefore, sliding motion between both discs is neglected and no friction force is present at the point of contact.

3.3 Point contact before loading

The vertical distance between two arbitrarily corresponding points lying on the surfaces of the bodies and on a line normal to the common tangent $x - y$ plane near the point of contact is required for contact area calculation [43]. Figure 3-2 shows the corresponding points and the vertical distance between them.

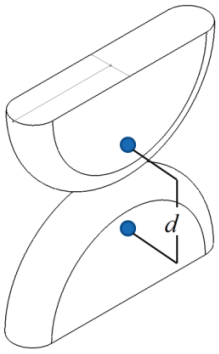

Figure 3-2: Corresponding points

The distance between each point to the tangent plane is expressed by z_1 for the first body and z_2 for the second where

$$\begin{bmatrix} z_1 \\ z_2 \end{bmatrix} = \begin{bmatrix} f_1(x,y) \\ f_2(x,y) \end{bmatrix} \tag{3-1}$$

The total vertical distance between both points before loading is approximated by [41]

$$d = z_1 + z_2 = f(x,y) \tag{3-2}$$

Note that the total vertical distance is the separation distance between the points. The equation that approximates the total separation distance between the points is approximated by

$$d = Ax^2 + By^2 \tag{3-3}$$

where x and y are coordinates with the origin at the point of contact O_{xyz} and the constants A and B depend on the principal radii of curvature of both discs at the point of contact and defined

by Equations (3-4) and (3-5) [43]. Note that the values of A and B are related to the geometric shape and configuration of the two discs, as given below:

$$A = \frac{1}{4}\left(\frac{1}{R_1}+\frac{1}{R_2}+\frac{1}{R_1'}+\frac{1}{R_2'}\right) - \frac{1}{4}\sqrt{\left[\left(\frac{1}{R_1}-\frac{1}{R_1'}\right)+\left(\frac{1}{R_2}-\frac{1}{R_2'}\right)\right]^2 - 4\left(\frac{1}{R_1}-\frac{1}{R_1'}\right)\left(\frac{1}{R_2}-\frac{1}{R_2'}\right)sin^2\,\emptyset} \tag{3-4}$$

$$B = \frac{1}{4}\left(\frac{1}{R_1}+\frac{1}{R_2}+\frac{1}{R_1'}+\frac{1}{R_2'}\right) + \frac{1}{4}\sqrt{\left[\left(\frac{1}{R_1}-\frac{1}{R_1'}\right)+\left(\frac{1}{R_2}-\frac{1}{R_2'}\right)\right]^2 - 4\left(\frac{1}{R_1}-\frac{1}{R_1'}\right)\left(\frac{1}{R_2}-\frac{1}{R_2'}\right)sin^2\,\emptyset} \tag{3-5}$$

3.4 Surface contact after loading

The result of force P is to cause elastic deformation of the discs over the region surrounding the initial point of contact. When the force P is applied, the point of contact becomes surface contact and continues to increase with increasing force. It is assumed that the boundary line of the contact surface forms an elliptic area between the discs as seen in Figure 3-3:

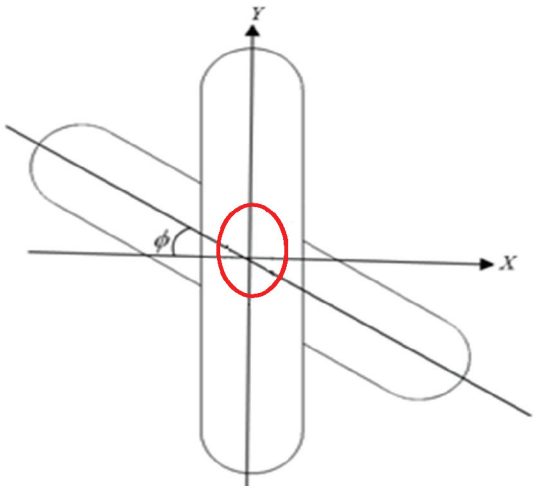

Figure 3-3: Contact area

The contact area follows the equation of an ellipse as described by:

$$\frac{x^2}{a^2}+\frac{y^2}{b^2}=1 \tag{3-6}$$

where x and y are coordinates with the origin at the point of contact; a is the semi-major axis of an ellipse and b is the semi-minor axis of the ellipse. Note that a and b are positive constants that determine the shape of the contact area between both discs. The task here is to determine the magnitude of the semi-major and semi-minor axes. They are related by the constant k where

$$k=\frac{b}{a} \tag{3-7}$$

The semi-minor axis b is determined by [43]:

$$b=\sqrt[3]{\frac{3kE(k')}{2\pi}(F\Delta)} \tag{3-8}$$

Where F is the applied compressive force,

$$\Delta=\frac{1}{A+B}\left(\frac{1-\upsilon_1^2}{E_1}+\frac{1-\upsilon_2^2}{E_2}\right) \tag{3-9}$$

In Equation (3.9), υ_1 and υ_2 are the Poisson's ratios of both discs and E_1 and E_2 are the modulus of elasticity.

Equation (3.8) is a function of only one unknown k and all other variable are determined from the physical properties of the discs. k is not determined by an exact solution but rather by an approximation using the following equation:

$$\frac{B}{A}=\frac{\left(\frac{1}{k^2}\right)E(k')-K(k')}{K(k')-E(k')} \tag{3-10}$$

Where A and B are determined from (3-4) and (3-5), and,

$$k' = \sqrt{1 - k^2} \tag{3-11}$$

In addition, $K(k')$ is the complete elliptic integral of first kind, expressed by:

$$K(k') = \int_0^{\frac{\pi}{2}} \frac{d\theta}{\sqrt{1 - k'^2 \sin^2 \theta}} \tag{3-12}$$

and $E(k')$ is the complete elliptic integral of second kind

$$E(k') = \int_0^{\frac{\pi}{2}} \sqrt{1 - k'^2 \sin^2 \theta}\, d\theta \tag{3-13}$$

Figure 3-4 is an approximated solution to (3-10) and it shows that B/A vs. k is a monotonic decreasing function. Thus, there must be a unique k value corresponding to each B/A value.

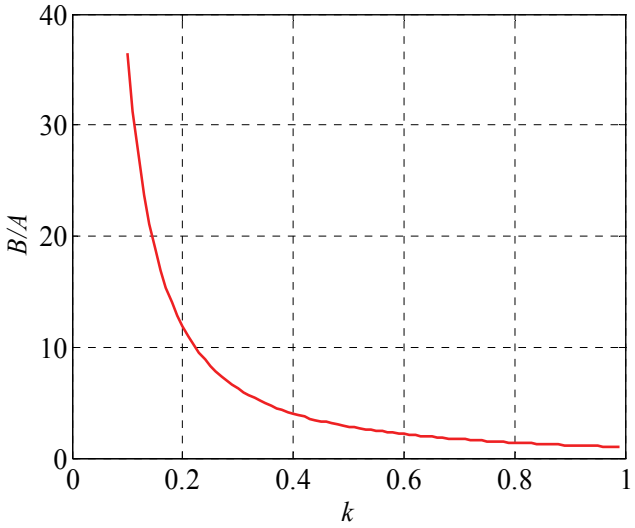

Figure 3-4: B/A vs. k

3.5 Frame of reference

The following section defines the frame of reference for contact area modeling. In general, the XYZ axis represents the global frame of reference and the xyz axis represents the local frame of reference. The local frame of reference is placed at the initial point of contact. Point N_{xyz} represents the origin of a rectangular coordinate system and the $x-y$ plane represents the tangent plane between the upper body B_1 and the lower body B_2 as seen in Figure 3-5. The directions of N_x and N_y are chosen for convenience to coincide with the axes of symmetry of the discs surfaces and N_z is chosen perpendicular to the $x-y$ plane.

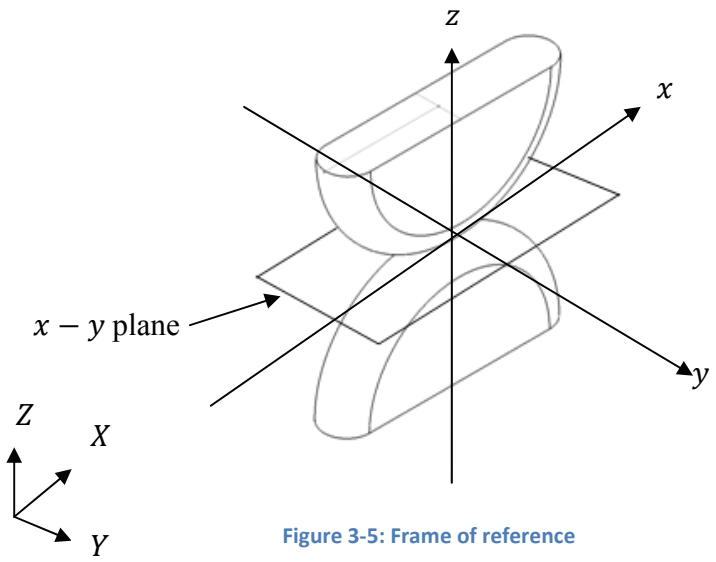

Figure 3-5: Frame of reference

With this introduction of Hertzian contact mechanics theory (emphasis on contact area) one may now substitute the polishing tool with the top disc and the part surface with the bottom disc. In the next chapter, the contact area theory is applied to consecutive contact points between the polishing tool and the part surface. For each contact point there is a corresponding contact area which is a function of the radius of curvature of the polishing tool and the part surface $\left(\text{i.e. } \forall N \; \exists \; CA(R_1, R_1', R_2, R_2')\right)$. Therefore, assuming that all model parameters area held fixed during the automated polishing process it is reasonable to infer that changes in radius of curvature results in changes in contact area. This is eventually how the contact area map was generated.

4 COVERAGE AREA MAP

Previous chapter introduced the Hertzian contact theory at a single contact point between two separate bodies under applied compressive force. The chapter ended by concluding that if all model parameters are held fixed (i.e. compressive force, modulus of elasticity, Poisson's ratio) then the contact area, generated between both bodies, is a function of only one variable: *radius of curvature* of both bodies. In the following chapter, the top body is substituted with the polishing tool and the bottom body is substituted with the part surface as proposed by Roswell [13]. This conclusion is applied to consecutive contact points along the part surface as to generate a polishing path that guarantees full coverage area.

The scope of the chapter is to develop a theory for generating a Coverage Area Map (*CAM*). To develop the theory, a series of contact points are defined along the part surface and used to develop a continuous polishing path with constant stepover size. In general, the Coverage Area Map is a two dimensional map that shows the contact area generated between the polishing tool and the part surface during robotic polishing process. In this chapter, the *CAM* is generated for:

1) A single discontinued raster path.
2) A continuous raster path with constant stepover size.

In subsequent chapters, it will be shown that the second case does not guarantee a full coverage of the part surface. Problems associated with the second case include under-polishing and over-polishing of the part surface. Thus, the polishing path has to be modified as to guarantee a full coverage of the part surface. The path is then modified by changing the stepover size for every contact point along the polishing path.

4.1 Coverage area map (*CAM*) for discontinued raster motion

Polishing tool-path (also referred as curves) is a path over the part surface to be polished, representing a strip that must be polished continuously. It is described by an ordered set of reference frames over the surface of the part to be polished. As discussed in section 3.5, the *z*-axis of each reference frame is always normal to the part surface at point N_{xyz}, and the x-axis points to the origin of the next reference frame [44].

For consistency throughout this work, let N represents a single contact point and CA the corresponding contact area. Recall from Chapter 3, that for any contact point N there a corresponding contact area CA which is a function of the radius of curvature $\left(\text{i.e. } \forall N \; \exists \; CA(R_1, R_1', R_2, R_2')\right)$. The contact area is generated when the applied compressive force deforms both bodies. The location of deformation is near the initial point of contact. The contact point N_i is located at the center of the contact area CA_i in the direction of desired tool-path as seen in Figure 4-1.

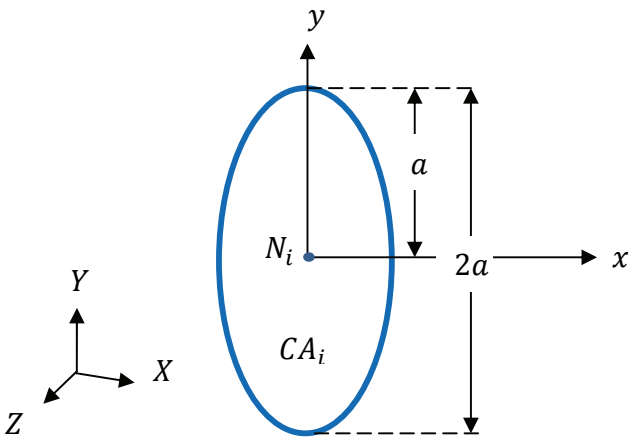

Figure 4-1: Contact area at point *N*

Generating polishing path P requires division of a continuous part surface into small discrete elements as to make it suitable for numerical evaluation and implementation on digital computers. P is a collection of distinct control points N_i generated by interpolating the discretized contact points along the part surface. In general, polishing flat surfaces requires minimum of two control points for generating a linear path $(i.e.\ N_1 \text{and } N_2)$; however, complex

surfaces require better control of the executed tool-path. Thus, multiple control points are introduced ($i.e.\ i \gg 2$). Therefore, P is described as follows:

$$P = \{N_1, N_2, \cdots, N_k, \cdots, N_i\} \qquad (4\text{-}1)$$

where N_i is the last contact point and N_k is the k^{th} contact point somewhere along the polishing path. Equation 4.1 is a polishing path for a single discontinued raster path. Figure 4-2 illustrates the process of discretizing continues part surface into small elements.

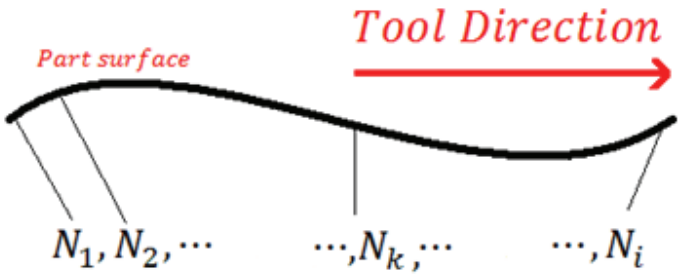

Figure 4-2: Discretizing arbitrary part surface

Every contact point N_i along the polishing path implies that a corresponding contact area CA_i exists at this point (i.e. $\forall N_i \Rightarrow \exists\ CA_i$). This brings us the introduction of the Coverage Area Map (CAM) as described for a single discontinued raster path by the following equation:

$$CAM = \{CA_1 \quad CA_2 \quad \cdots \quad CA_k \quad \cdots \quad CA_i\} \qquad (4\text{-}2)$$

Where

$$CA_i = \left\{ (x, y) \;\middle|\; \left(\frac{x^2}{a_i^2} + \frac{y^2}{b_i^2} = 1 \right) \right\} \qquad (4\text{-}3)$$

Equation (4-2) indicates that the Contact Area Map (CAM) is a set of Contact Areas (CA_i) where according to Equation (4-3), CA_i is the elliptic contact area generated between the polishing tool and the part surface for the i^{th} discretized point along the polishing path. The coordinates of x and y are defined in the local frame of reference in Figure 3-5. a_i and b_i are the

semi-major and semi-minor axes of the ellipse which are calculated from the radius of curvature of the polishing tool and the part surfaces as discussed in Chapter 3.

Figure 4-3 shows the Coverage Area Map (*CAM*) for a single discontinued raster path at multiple contact points. This is a special case of *CAM* since all the contact points along the path are in a straight line and all contact area have at the same length indicating constant semi-major axis. Note that for every contact point N_i there is a corresponding elliptic contact area that follows Equation (4-2).

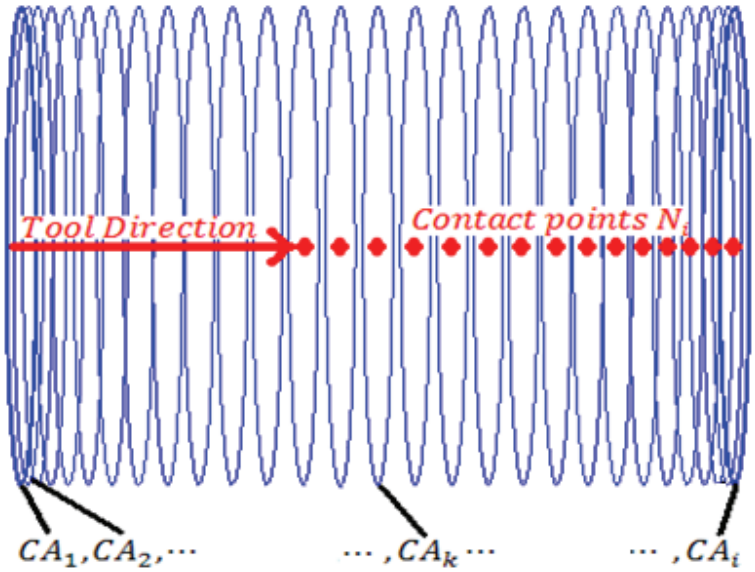

Figure 4-3: Coverage area for a discontinued raster path

The semi-minor axis b_i has no effect in generating the Coverage Area Map. Therefore, the *CAM* for a polishing path is a function of the semi-major axis a_i only.

$$CAM = f(a_1 \quad a_2 \quad \cdots \quad a_k \quad \cdots \quad a_i) \tag{4-4}$$

This conclusion is utilized in subsequent chapter when the continuous raster path is modified to generate a polishing path that guarantees full coverage area. In the mean time, recall that the semi-major axis a_k is a function of the radius of curvature as discussed in Chapter 3.

4.2 Coverage area map (*CAM*) for continuous raster motion

Section 4.1 introduced the theory for generating a Coverage Area Map (*CAM*) for a single discontinued polishing path. In the following section the theory is extended to cover a continuous raster polishing path. In general, a continuous raster polishing path is a set of all the paths along the part surface as described by the following equation:

$$CRP = \{P_1, P_2, \cdots \quad P_l \quad \cdots P_j\}^T \tag{4-5}$$

where CRP stands for continuous raster path. P_j represents the last polishing path and P_l represent the l^{th} polishing path somewhere along the part surface. Substituting Equation (4-1) into Equation (4-5) and recalling that every contact point N_{il} implies that there must be a corresponding contact area CA_{il} at this point (i.e. $\forall N_{il} \Rightarrow \exists\, CA_{il}$) results in the following equation:

$$CAM = \begin{Bmatrix} CA_{11} & CA_{21} & \cdots & CA_{i1} \\ CA_{12} & CA_{22} & \cdots & CA_{i2} \\ \vdots & \vdots & \cdots & \vdots \\ CA_{1l} & CA_{2l} & \cdots & CA_{il} \\ \vdots & \vdots & \ddots & \vdots \\ CA_{1j} & CA_{2j} & \cdots & CA_{ij} \end{Bmatrix} \tag{4-6}$$

Where l represents the l^{th} polishing path and i represents the i^{th} discretized point along the part surface. Once again, recall from Chapter 3 that the contact area is a function of the radii of curvatures of the part and the polishing tool. Thus, changes to the radii of curvatures results in changes to the contact area. Figure 4-4 shows the Coverage Area Map for a flat surface where the radii of curvatures is maintained constant. This is a special case of *CAM* since that the contact area remains constant $(i.e. CA_{il} = CA_{il+1}$ etc.$)$ throughout the part surface. In addition, the contact area is circular indicating that the semi-major axis and semi-minor axis area equal or nearly equal. Therefore, the stepover size between two consecutive paths remains constant as well (i.e. the vertical distance between centers of CA_{ik} and CA_{ik+1}). Note that in practice the contact area should be denser for every path. However, for illustration purposes, the contact areas were placed farther away from each other.

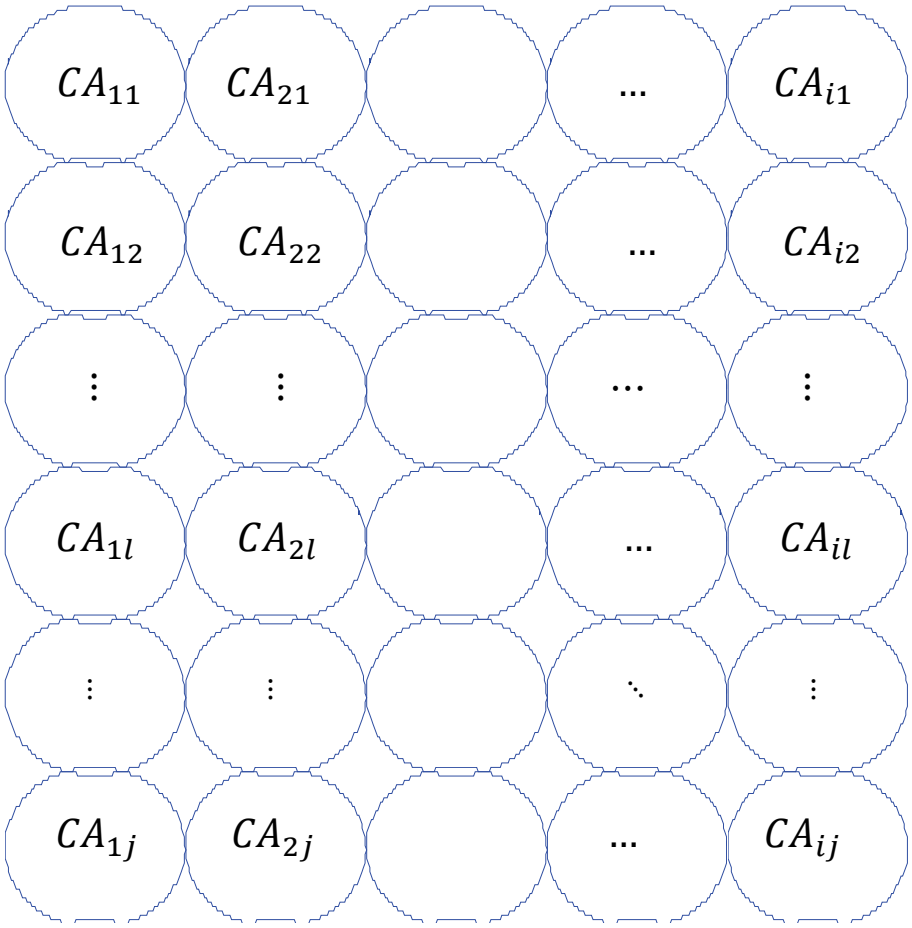

Figure 4-4: Coverage Area Map for a flat surface

In general, the stepover size between path P_l to an adjacent path P_{l+1} depends on the vertical distance between the contact area CA_l and CA_{l+1}. The vertical distance of the contact area in Figure 4-4 is defined as twice the semi-major axis $(i.e. 2a_{il})$. Thus, the stepover size between P_l to P_{l+1} should have a maximum vertical distance of $2a_{il}$ and the equation representing the Contact Area Map (4-6) is alternatively written in terms of the semi-major axis a:

$$CAM = \begin{Bmatrix} 2a_{11} & 2a_{21} & \cdots & 2a_{i1} \\ 2a_{12} & 2a_{22} & \cdots & 2a_{i2} \\ \vdots & \vdots & \cdots & \vdots \\ 2a_{1l} & 2a_{1l} & \cdots & 2a_{il} \\ \vdots & \vdots & \ddots & \vdots \\ 2a_{1j} & 2a_{2j} & \cdots & 2a_{ij} \end{Bmatrix} \tag{4-7}$$

In Chapter 5 the continuous raster path with constant stepover size is applied to three different part surfaces and the coverage area map (*CAM*) is generated in each case. It will be shown that constant stepover size results in undesired effects during polishing. The effects are influenced by the stepover size and they are as follows:

3) Large stepover size: an envelope of unpolished region is generated between the paths. This envelope indicates that the polishing tool did not come in contact with the part at this region and it results in a rough surface. In this case, additional paths are required as to remove the rough surface and guarantee full coverage during polishing.

4) Small stepover size: results in overlapping between adjacent paths. Overlapping may degrade the part surface and decrease polishing tool life as the same area is covered more than once. This results in increased production time and manufacturing costs.

In subsequent chapters, Equation (4-7) is utilized for generating a modified polishing path that overcomes these unwanted effects and guarantees full coverage area during robotic polishing.

5 POLISHING PATH: CONSTANT STEPOVER SIZE

In Chapter 4 the theory of Coverage Area Map (*CAM*) is introduced. Recall that, the *CAM* was generated based on Hertzian contact theory to model the interaction between the polishing tool and the part surface for consecutive points along the part surface. In general, the *CAM* is a two dimensional map that shows the contact area generated between the polishing tool and the part surface during robotic polishing process. The map is first generated for a single discontinued raster path and later it is extended to continuous raster path along the part surface. In the following chapter, the *CAM* is generated for various surfaces with constant stepover size. It is shown that polishing paths with constant stepover size do not guarantee full coverage of the part surface. Herein, three different scenarios are simulated and they are as follows:

4) Two fixed radii of curvatures (i.e. flat surfaces)
5) One fixed and one varying radii of curvature (i.e. semi-spherical tube)
6) Two varying radii of curvature (i.e. ellipsoid)

In subsequent chapters the *CAM* is utilized to modify the polishing path and eliminate the problems associated with polishing path with constant stepover size introduced in this chapter.

5.1 Polishing tool

In the scope of this research, the polishing tool under study is assumed to carry a semi-spherical polishing head where the tip of the tool is tangent to the part surface and its centerline is normal to the part surface. From these assumptions the following two conclusions are made:

1. The minimum and maximum radii of the polishing tool are equal ($i.e. R_1 = R_1'$).
2. The angle between planes of principal curvature is equal to zero ($i.e. \emptyset = 0$).

5.2 Part with two fixed radii of curvatures

Figure 5-1 shows the setup for this simulation where the part has a flat surface. This is a special case for generating the Coverage Area Map (*CAM*) for the following reasons:

1. Constant part surface: implies that there is no change to the part's radii of curvatures.
2. Minimum and maximum radii of curvatures approaching infinity ($R_2 = R_2' = \infty$).

Recall from Chapter 3 that the contact area is a function of the radii of curvatures of the part and the polishing tool. Thus, changes to the radii of curvatures results in changes to the contact area. As per first assumption, no change in radii of curvature implies that the *CAM* is uniform throughout the part surface.

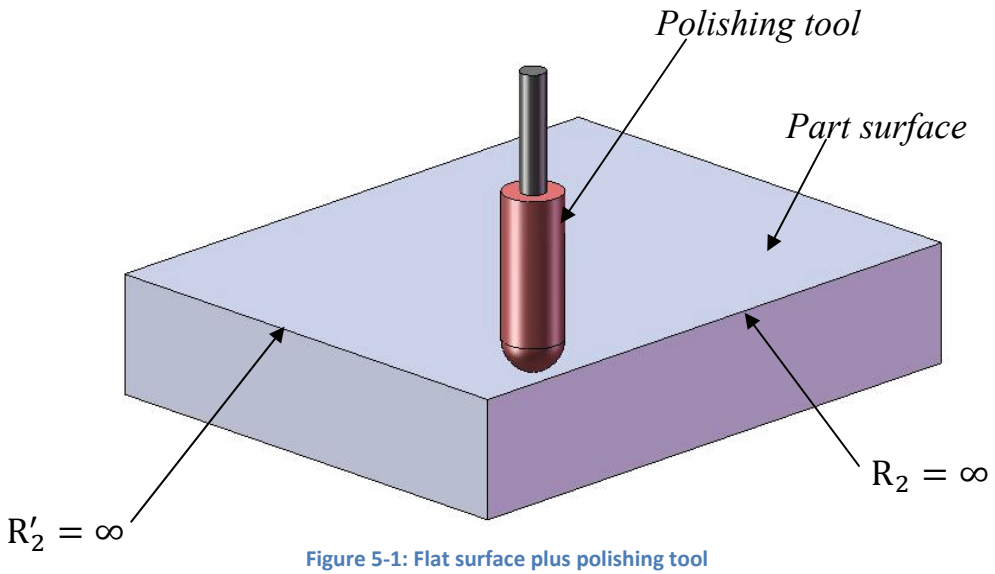

Figure 5-1: Flat surface plus polishing tool

Figure 5-2 shows a conventional continuous raster path on a flat surface. The path is highlighted in red. Notice that the tool engages at a starting point and go back and forth along the part surface with constant stepover size between two adjacent paths.

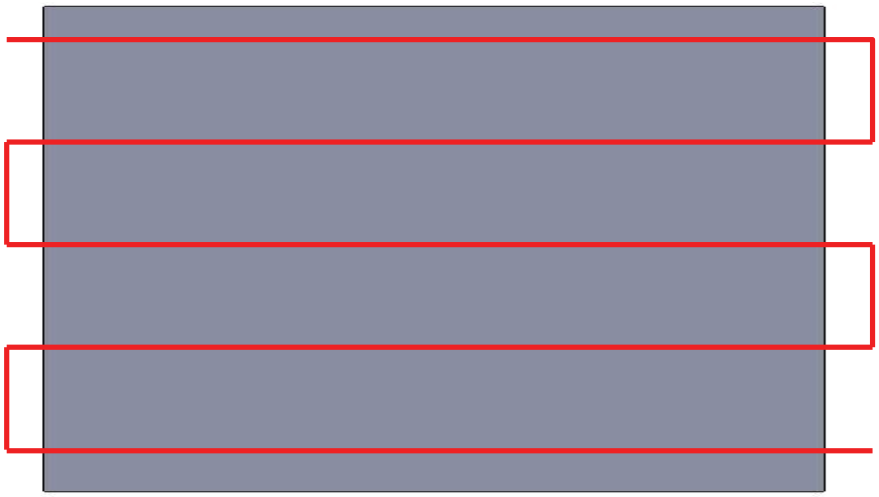

Figure 5-2: Flat surface with continuous raster path

Figure 5-3 shows k versus tool location along the part surface for a single discontinued raster path. Note that k is constant throughout the path indicating that a/b ratio is constant. In addition, $k = 1$ indicates that the semi-major axis a equals the semi-minor axis b which implies that the contact area is circular (*i.e.* special case of an ellipse).

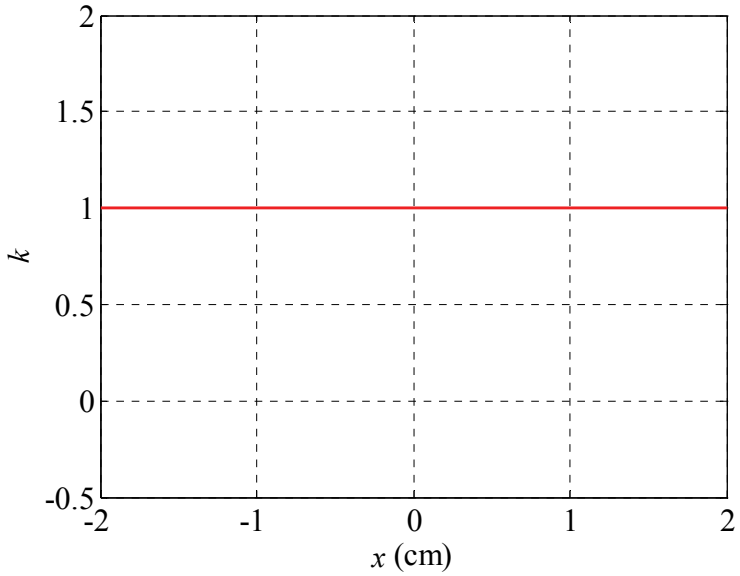

Figure 5-3: *k vs. tool location*

Figure 5-4 represents the semi-major axis a and semi-minor axis b versus tool location x. Note that both a and b are constants indicating that the contact area is fixed throughout the part surface. Since $a = b$ it implies that contact area is circular.

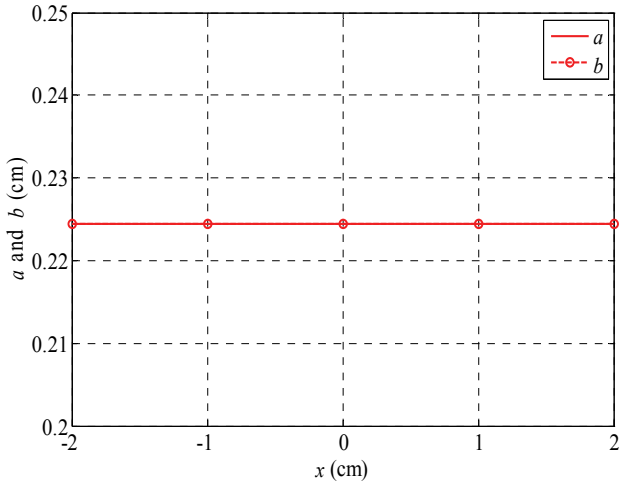

Figure 5-4: Semi-major and semi-minor axes vs. tool location

Figure 5-5 shows the position of the center of the polishing tool as a function of the stepover size versus tool location. Recall that the contact area is a function of the semi-major axis. Since the semi-major axis is constant throughout the part surface the stepover size between adjacent paths is also constant.

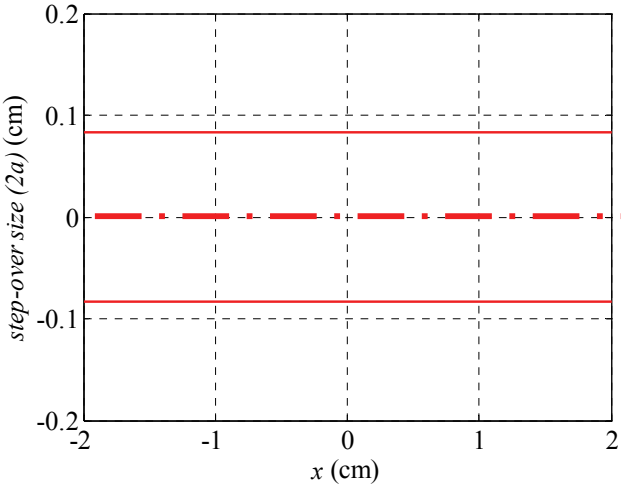

Figure 5-5: Stepover size vs. tool location

Next, the Coverage Area Map (CAM) is generated for the flat surface with constant stepover size. Figure 5-6 shows an ideal Coverage Area Map for the flat surface where the radii of curvatures is maintained constant. Note that the stepover size between two adjacent paths remained uniform throughout the part surface. This is a result of uniform contact area as predicted in prior analysis. This case represents a full coverage area between adjacent paths.

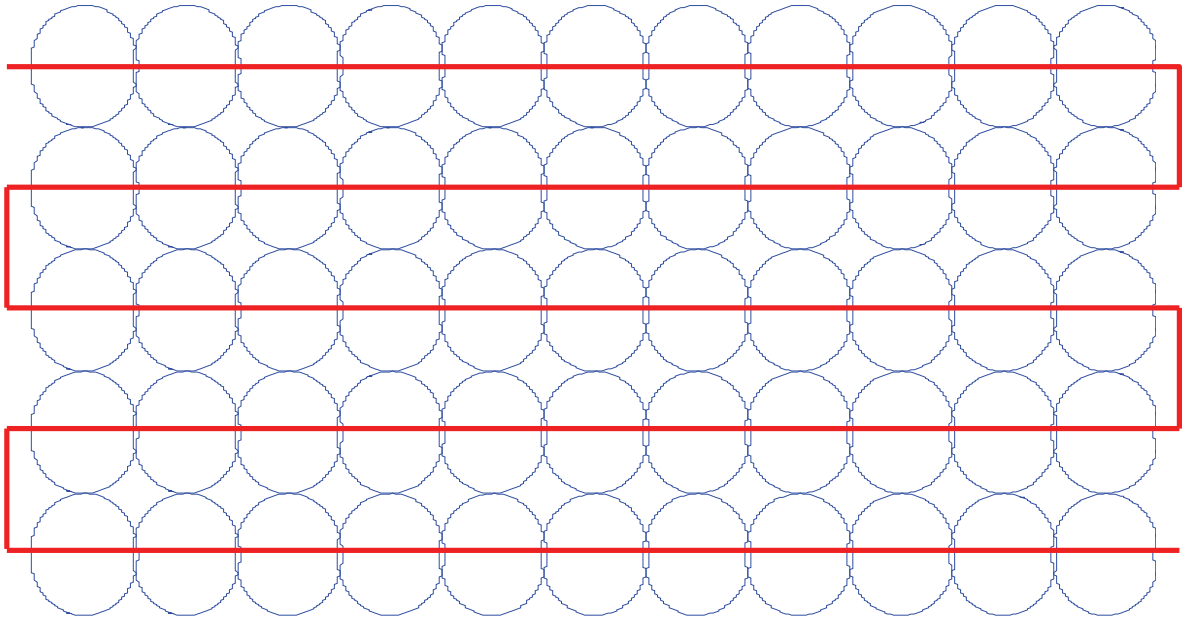

Figure 5-6: Coverage area map for a flat surface

NOTE: Flat surface is a special case of *CAM* where the radii of curvatures of the part surface approaches infinity resulting in constant contact area throughout the surface.

Theoretically though, the continuous raster path (highlighted in red) is not an efficient method for generating polishing paths. Its inefficiency is shown next for two cases: large stepover size and small stepover size.

CASE I: Large stepover size:

Figure 5-7 shows the *CAM* for the flat surface with constant stepover size of 2.2 mm between adjacent paths. Large stepover size was selected to show the effect of the unpolished area generated between adjacent paths. The unpolished area, highlighted in green, represents a region where the polishing tool does not come in contact with the part surface.

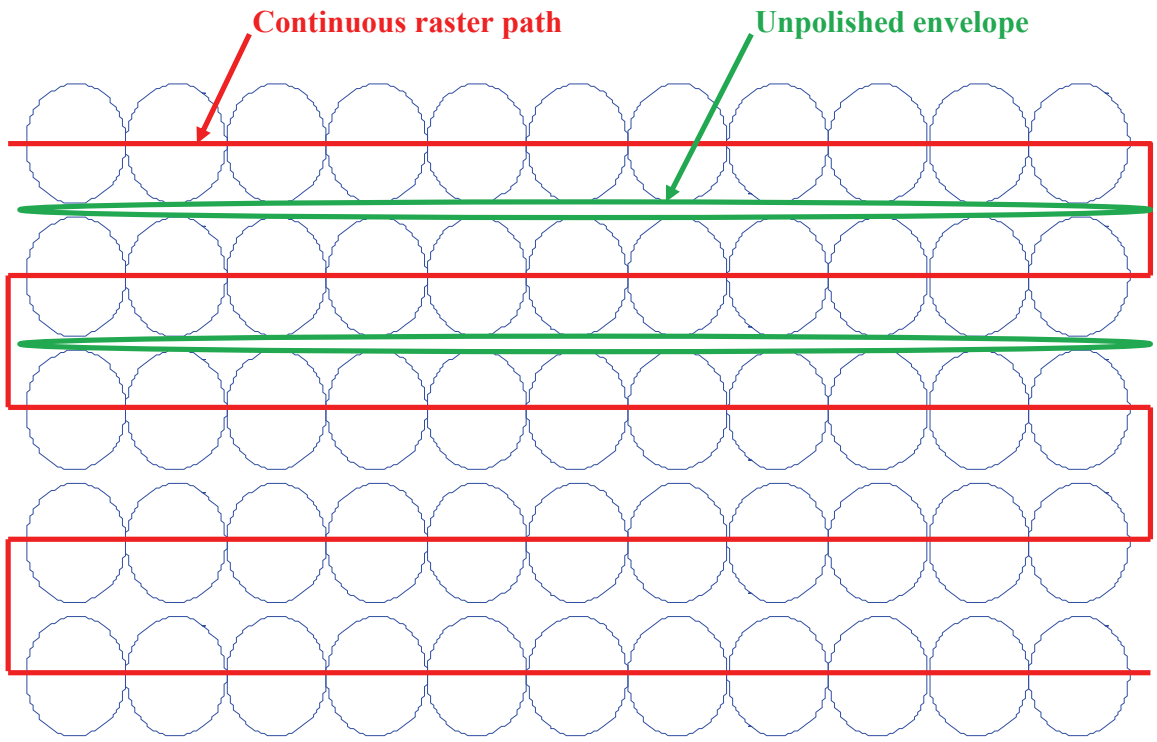

Figure 5-7: Flat surface with large stepover size

CASE II: Small stepover size:

Figure 5-8 shows the *CAM* for the flat surface with constant stepover size of 1.6 mm between adjacent paths. Small stepover size was selected to show the crowding effect generated between adjacent paths. The crowding effect, highlighted in green, represents a region where the polishing tool overlaps the same path more than once. This results in inefficient robotic polishing as many paths have to be designed to cover the same area which results in high production time and undesired manufacturing costs.

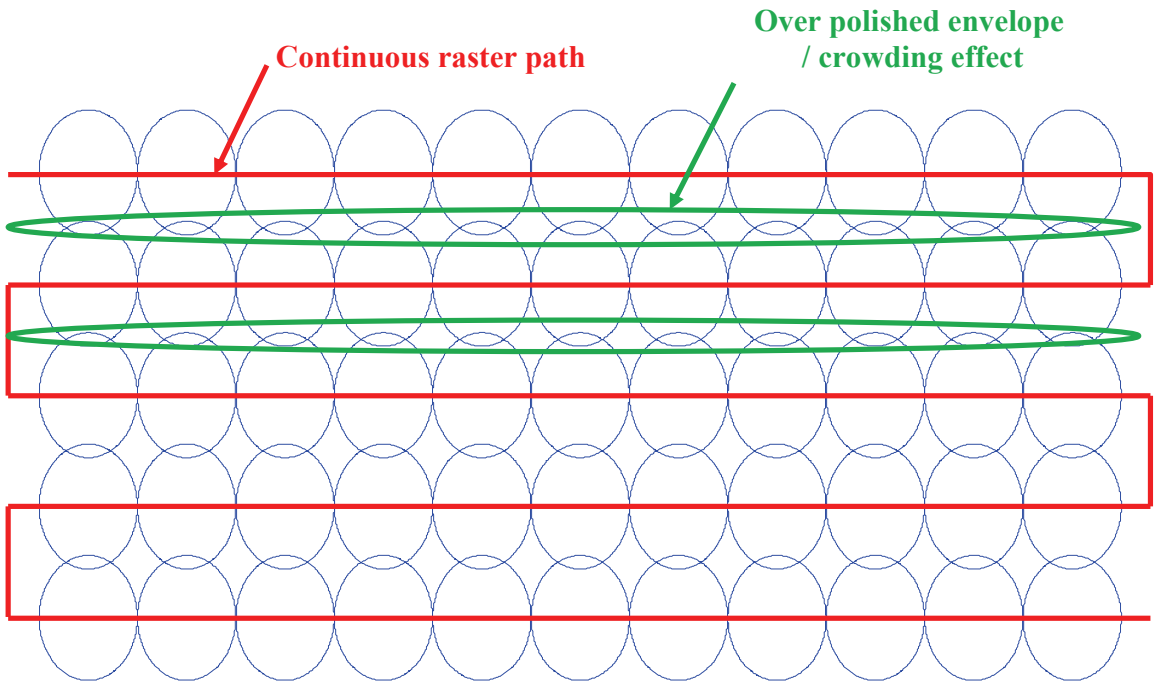

Figure 5-8: Flat surface with small stepover size

For flat surfaces the stepover size is constant between adjacent paths and the computation is relatively easy. The next example is more involved and show changes in the contact areas along the polishing path as the radii of curvatures changes. This results in non- uniform coverage area.

5.3 Part with one fixed and one changes radii of curvatures

Figure 5-9 shows the setup for this simulation where the part surface is semi-elliptic tube with semi-major axis $a = 20cm$ and semi-minor axis $b = 10cm$ as indicated. Figure 5-10 shows an isometric view of the polishing tool and the part surface. The radii of curvatures of the part surface changes in one direction while the other is kept constant. Therefore, the following conclusion is made:

The minimum radius of curvature of the part surface approaches infinity ($i.e.\ R_2 = \infty$).

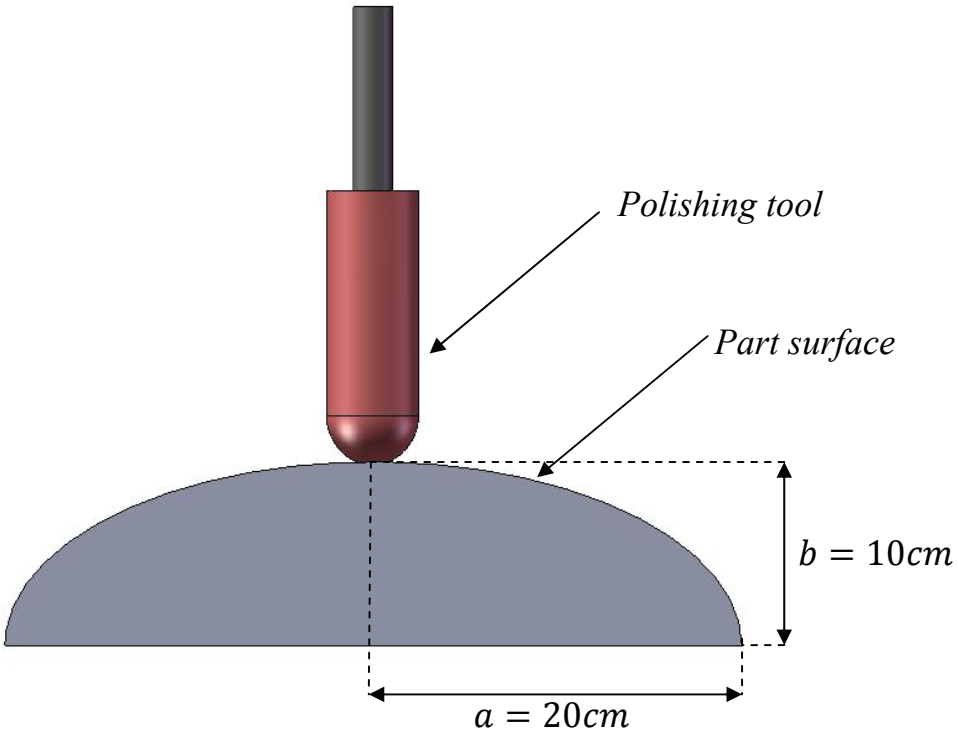

Figure 5-9: Semi-elliptic tube plus polishing tool - Front view

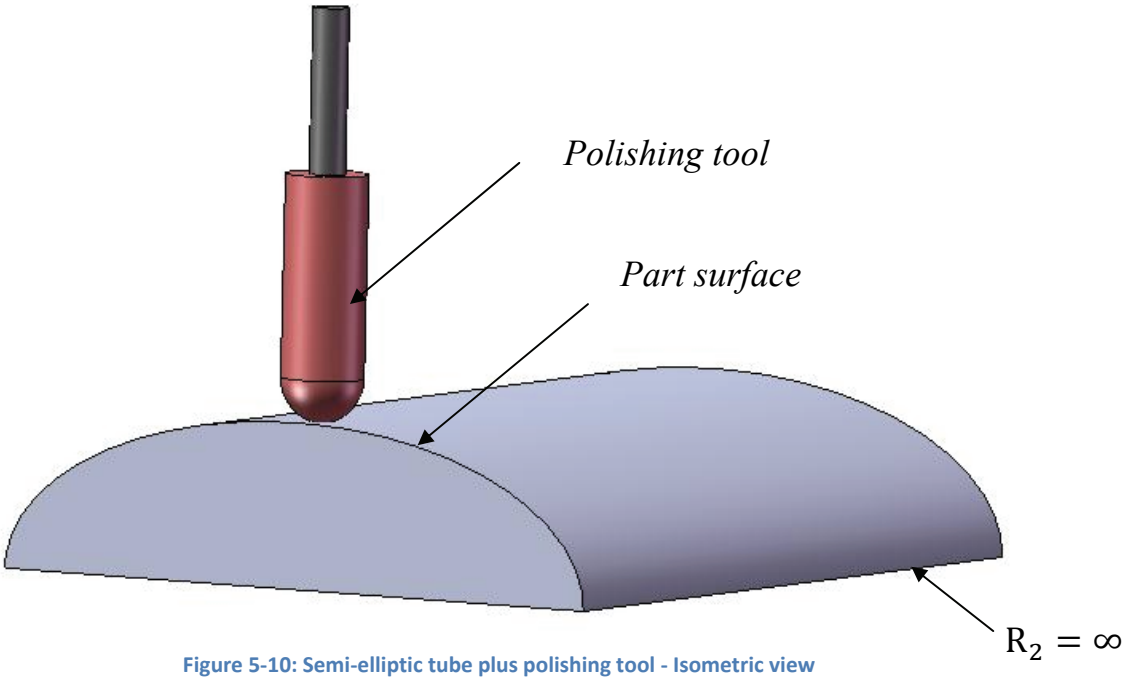

Figure 5-10: Semi-elliptic tube plus polishing tool - Isometric view

With the assumptions of the polishing tool made in Section 5.1 ($i.e. R_1 = R_1'$ and $\emptyset = 0$) and the assumption that the minimum radius of curvature of the part approaches infinity ($i.e.\ R_2 = \infty$) Equation (3-4) reduces to

$$A = \frac{1}{2R_1} \tag{5-1}$$

Equation (5-1) indicates that A is a function of the principal radii of the polishing tool only. This implied that A is constant since that the principal radius of the polishing tool is assumed to be constant. The same assumptions are applied to (3-5) in which the equation reduces to

$$B = \left(\frac{1}{2}\right)\left(\frac{1}{R_1} + \frac{1}{R_2'}\right) \tag{5-2}$$

Equation (5-2) implied that B is a function of the radii of curvatures of both the polishing tool and the part surface. If R_1 is constant then B is a function of R_2' only. It is shown later that

changes in A and B results in changes to the semi-major a and semi-minor b of the contact area. Therefore, the coverage area changes along the part surface.

The maximum radius of curvature R_2' is calculated with the following equation:

$$k = \frac{|x'y'' - y'x''|}{\left(x'^2 + y'^2\right)^{\frac{3}{2}}} \tag{5-3}$$

Equation (5-3) is the general equation for computing radius of curvature. Where $x', x'', y', \text{and } y''$ are the first and second derivatives of x and y. For the case of an ellipse $x = a\cos\theta$ and $y = b\sin\theta$. Where a and b are the semi-major and semi-minor axes of the part surface. Equation (5-4) is the radius of curvature of an ellipse

$$k = \frac{ab}{(b^2\cos^2\theta + a^2\sin^2\theta)^{\frac{3}{2}}} \tag{5-4}$$

The part has a semi-elliptic surface with symmetry along its main axis. The radius of the profile increases from both ends towards the center of the part. Figure 5-11 shows the radius change versus location of the polishing tool. The maximum radius occurs at the center where $x = 0$ and the minimum radius at both ends where $x = \pm 20(cm)$.

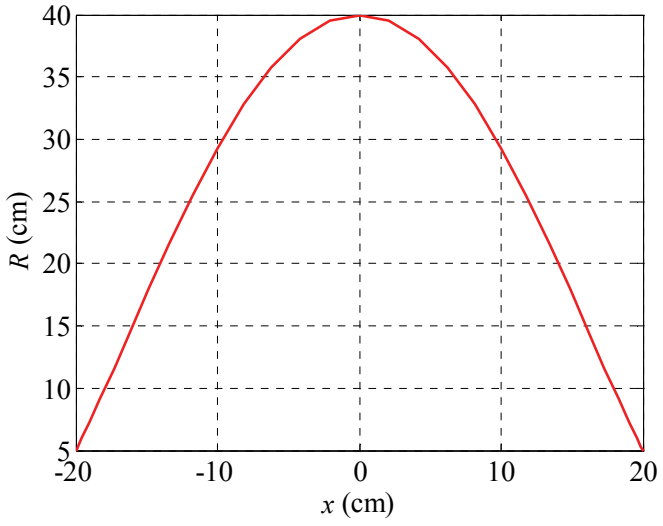

Figure 5-11: maximum part radius vs. tool location

From Equations (5-1) and (5-2), the ratio B/A is a function of R_1 and R_2'. Since R_1 is constant, B/A is a function of R_2' only. As R_2' increases B/A decreases and vice versa, as R_2' decreases B/A increases. The change in radius affects the semi-major and semi-minor axes of the contact area between the polishing tool and the part surface. This discussion leads to important observations with regards to the contact area.

1. $R \uparrow \Leftrightarrow R_2' \downarrow$ Increase in part radius indicates decrease in radius of curvature.
2. $R_2' \downarrow \Leftrightarrow B/A \downarrow$ Decrease in radius of curvature indicates decrease in B/A.
3. $B/A \downarrow \Leftrightarrow k \uparrow$ Decrease in B/A indicates increase in k (Figure (3-3)).
4. $k \uparrow \Leftrightarrow b/a \uparrow$ Increase in k indicates increase in b/a (Equation (3-7))
5. $b/a \uparrow \Leftrightarrow CA \uparrow$ Increase in b/a indicates increase in contact area ($0 \leq b/a \leq 1$).

Therefore, increase in part radius results in large contact area. Figure 5-12 shows a graph of k vs. tool location along the part surface. The following observations are made:

1. At $x = 0(cm)$ (MaximumR_2'): k approaches unity which implies that the contact area at this region resembles a circular contact area.
2. At $x = \pm 20(cm)$ (MinimumR_2'): small k indicates elliptic contact area at these points.

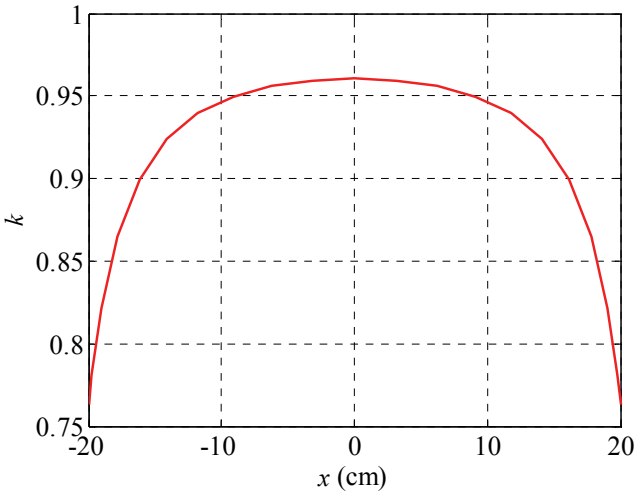

Figure 5-12: *k* value vs. tool location

SPECIAL CASE: $k = 1$ implies that the semi-major and semi-minor axes are equal indicating that the equation of an ellipse reduces to the equation of a circle and the contact area is circular.

Figure 5-13 shows a plot of the semi-major axis a and semi-minor axis b of the elliptic contact area versus tool location. The following observations are made:

1. At $x = 0$: The vertical distance between a and b is small indicating that k is closer to unity. Thus, the contact area resembles a circle (i.e. no longer elliptic)
2. At $x = \pm 20(\text{cm})$: The vertical distance between a and b is large indicating that b/a is small which implies that the contact area is elliptic.

This figure indicates that for parts with curved profiles the contact area between the polishing tool and the part surface changes with the radius of curvature of the part.

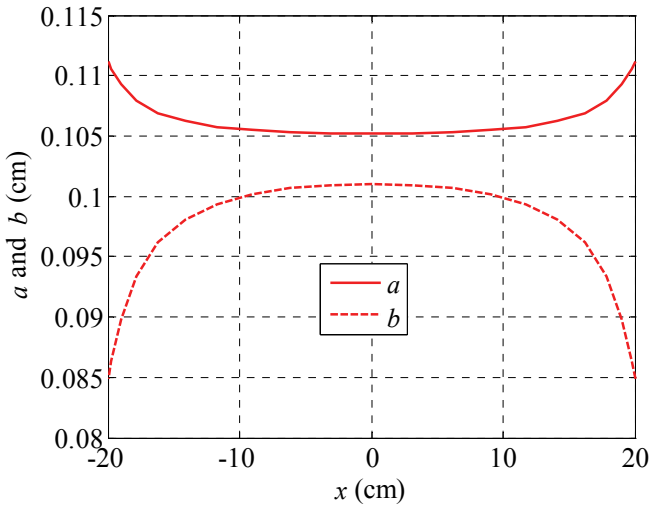

Figure 5-13: major-axis and minor axis vs. tool location

The discussion resulted in two conclusions with respect to the contact area between the polishing tool and the part surface. The conclusions are as follows:

1) Increase in part radius (*i.e.* small radius of curvature) implies that the contact area between the polishing tool and the part profile increases.

$$Part\ radius\ increases \Longrightarrow Contact\ area\ increases$$

2) Decrease in part radius (*i.e.* large radius of curvature) implies that the contact area between the polishing tool and the part profile decrease.

$$Part\ radius\ decreases \Longrightarrow Contact\ area\ decreases$$

Based on the previous discussion, the Coverage Area Map (*CAM*) is generated for this part. The following two observations area made:

1. At $x = 0(cm)$: Large profile radius (*i.e.* small radius of curvature) indicating large contact area.
2. At $x = \pm 20(cm)$: Small profile radius (*i.e.* large radius of curvature) indicates that small contact area.

The coverage area is determined by generating two envelope lines at the boundary of the polishing path in as seen in Figure 5-14. The boundary lines are represented by the semi-major axis a. The area generated in the boundary lines represents the coverage area that the polishing tool covered during a single discontinues raster path along the part surface.

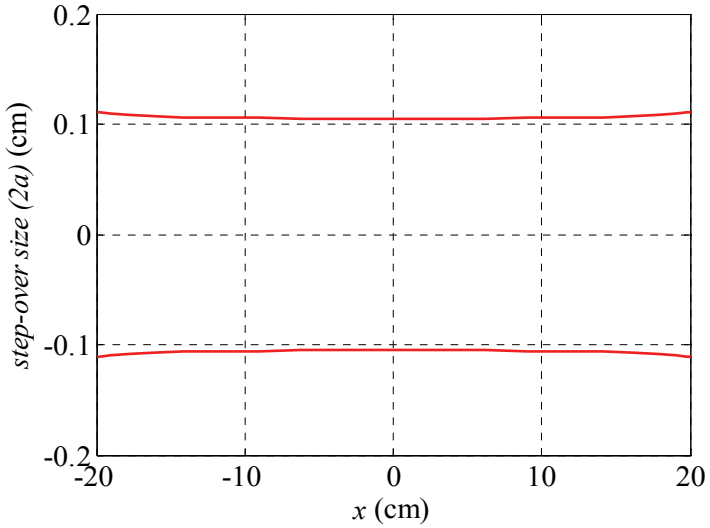

Figure 5-14: Coverage area for a single discountinued path

Note that the boundary lines of the coverage area are not straight lines. This is as a result of the change in the radius of curvature along the part profile. Recall from Chapter 3 that the contact area is a function of the radii of curvatures of the part and the polishing tool. Thus, changes to the radii of curvatures results in changes to the contact area.

The same procedure as outlined in previous section is applied here. The continuous raster path, highlighted in red, is shown for two cases: large stepover size and small stepover size.

CASE I: Large stepover size:

Figure 5-15 shows the *CAM* for the part surface with constant stepover size between adjacent paths. The polishing path is planned with the stepover size larger than the polishing tool diameter. Large stepover size was selected to show the effect of the unpolished area generated between the paths. The unpolished area, highlighted in green, represents a region where the polishing tool does not come in contact with the part surface. The part profile is semi-elliptic with semi-major axis $a = 2cm$ and semi-minor axis $b = 1cm$. Note that to cover the entire part surface six tool path were required.

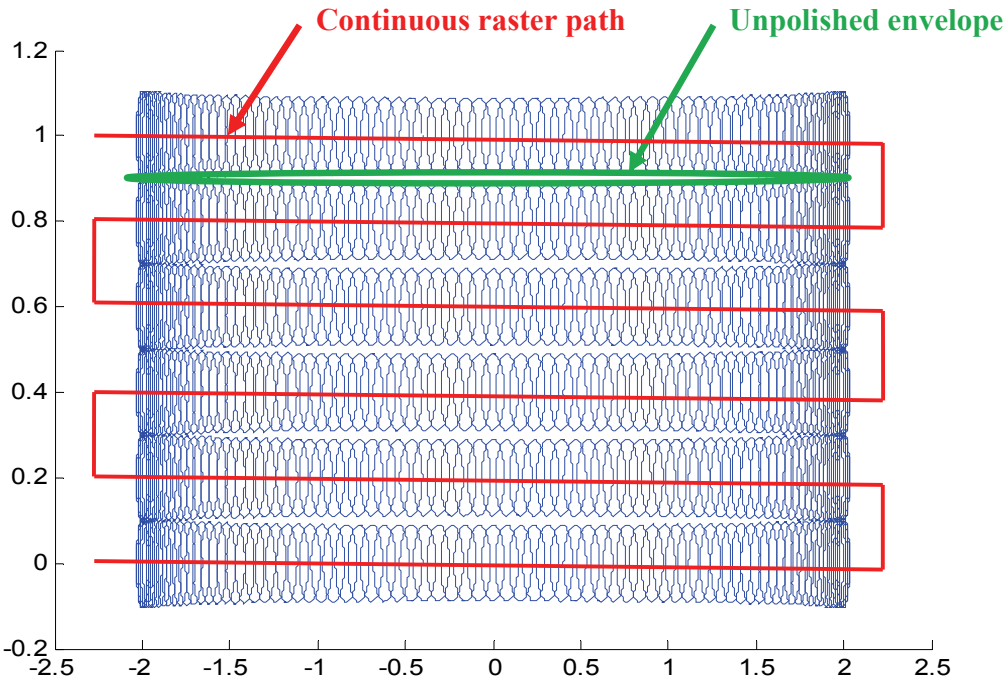

Figure 5-15: Large stepover size

CASE II: Small stepover size:

Figure 5-16 shows the *CAM* for the part surface with constant stepover size between adjacent paths. Small stepover size was selected to show the crowding effect generated between the paths. The crowding effect, highlighted in green, represents a region where the polishing tool overlaps the same contact area more than once. This results in inefficient robotic polishing as many paths have to be designed to cover the same area which results in high production time and undesired manufacturing costs. The part profile is semi-elliptic with semi-major axis $a = 2cm$ and semi-minor axis $b = 1cm$. Note that to cover the entire part surface seven tool path were required.

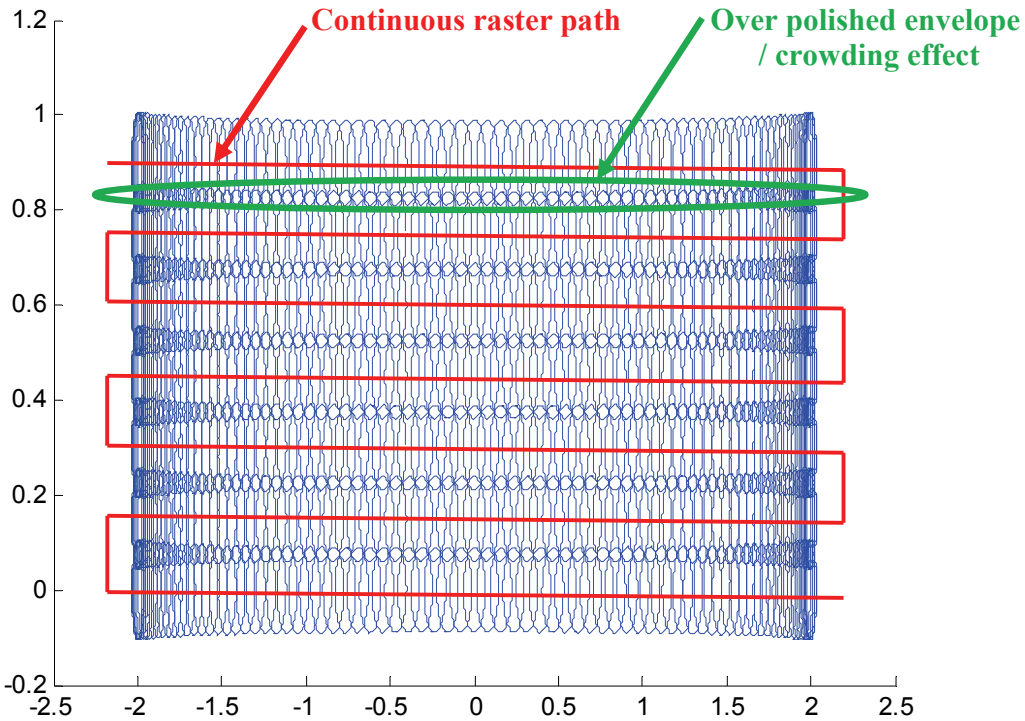

Figure 5-16: Small stepover size

Figure 5-15 and Figure 5-16 show the problems associated with conventional continuous raster path. In the first case, the Coverage Area Map (*CAM*) shows that the part surface is not completely polished. In the second case, however, the polishing path overlaps the same region more than once. Therefore, the polishing path has to be modified to overcome these problems. Optimal polishing path can be achieved if the stepover size would be determined by the semi-

major axis at each contact point. This approach is brought up in subsequent chapters as a solution that guarantees a full coverage area of the part surface during robotic polishing.

Up to this point the Coverage Area Map (*CAM)* was generated for two part surfaces. The first part is a special case of the coverage area map where the radii of curvatures are maintained constant throughout the part surface. The second part had one constant radius of curvature while the other changes throughout the part surface. In the next section, the Coverage Area Map (*CAM*) is generated for a part with two radii of curvature that changes in all directions throughout the part surface.

5.4 Part with two changing radii of curvatures

In the following section, the Coverage Area Map (*CAM*) is generated for part surface where the radii of curvatures change in xz and yz planes. Figure 5-17 shows an isometric view of the part surface for this simulation. The general equation of an ellipsoid aligned at the origin of xyz Cartesian coordinate system is given by:

$$\frac{x^2}{a^2} + \frac{y^2}{b^2} + \frac{z^2}{c^2} = 1 \qquad (5\text{-}5)$$

where $a = 1(cm)$, $b = 0.6(cm)$ and $c = 0.8(cm)$ are fixed positive real numbers that determine the shape of the ellipsoid.

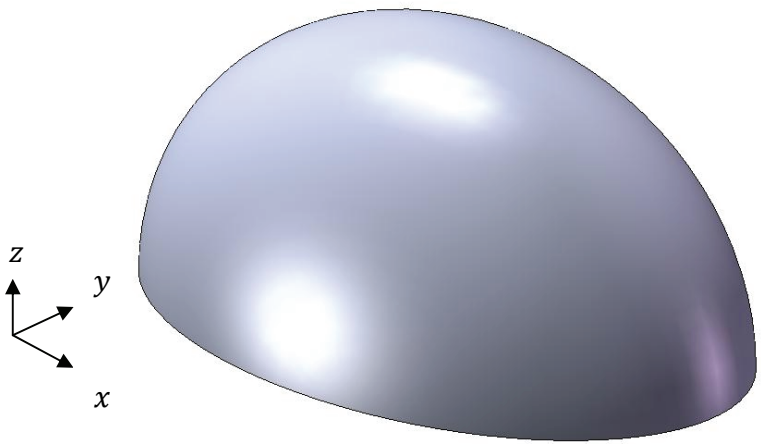

Figure 5-17: Semi-ellipsoid part surface

The radius of curvature in the xz plane is given by the following equation: (Appendix A)

$$K_{xz} = \frac{AC_{xz}}{\left(A^2\left(\frac{z^2}{c^2}\right)+C_{xz}^2\left(\frac{x^2}{a^2}\right)\right)^{\frac{3}{2}}} \tag{5-6}$$

where $A = \left[\frac{a^2(b^2-y^2)}{b^2}\right]$ and $C_{xz} = \left[\frac{c^2(b^2-y^2)}{b^2}\right]$

And the radius of curvature in the yz plane is given by the following equation:

$$K_{yz} = \frac{BC_{yz}}{\left(B^2\left(\frac{z^2}{c^2}\right)+C_{yz}^2\left(\frac{x^2}{b^2}\right)\right)^{\frac{3}{2}}} \tag{5-7}$$

where $B = \left[\frac{b^2(a^2-x^2)}{a^2}\right]$ and $C_{yz} = \left[\frac{c^2(a^2-x^2)}{a^2}\right]$

Because of the geometrical complexity of the problem, the part surface is divided into two separate sections. The Coverage Area Map (*CAM*) is generated for each section separately and then it is combined. Figure 5-18 shows the projection of the ellipsoid and both sections for the polishing path.

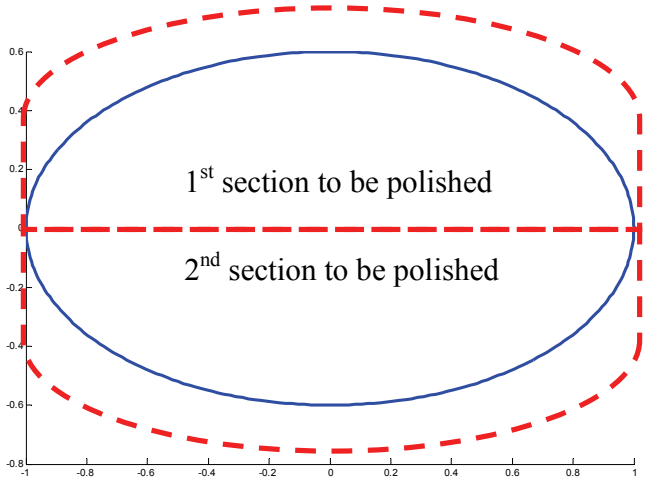

Figure 5-18: Projection of the ellipsoid

Figure 5-19 shows the projection of the ellipsoid with continuous raster polishing path, highlighted in red. Note that the stepover size is maintained constant between two adjacent paths throughout the part surface.

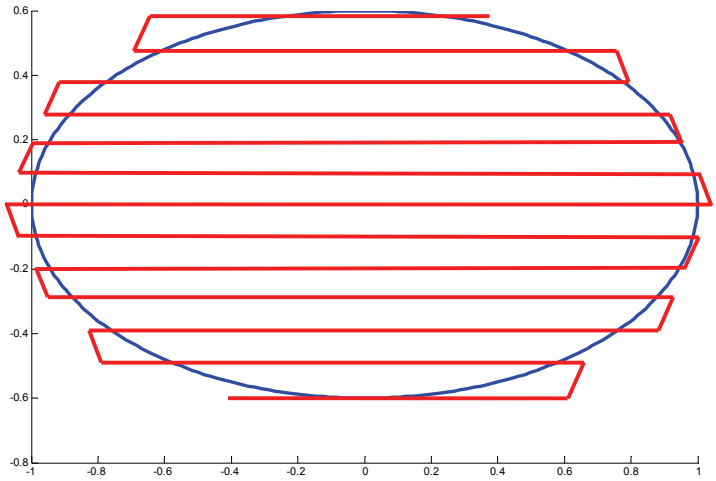

Figure 5-19: Raster polishing path with fixed stepover size for an ellipsoid

Figure 5-20 shows the Coverage Area Map (*CAM*) for the ellipsoid. The map was generated using the continuous raster path.

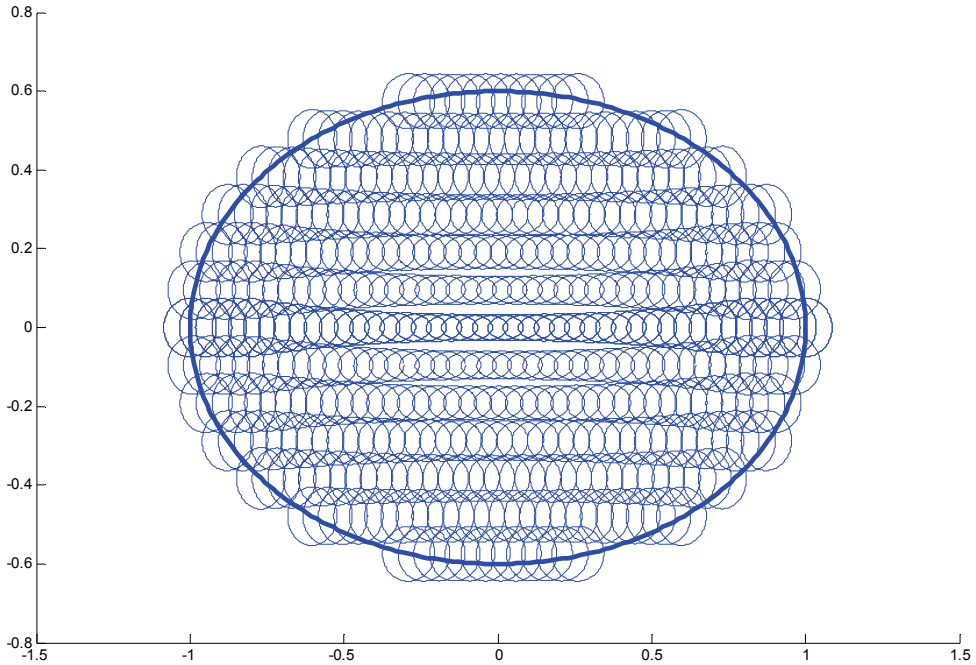

Figure 5-20: Polished ellipsoid with raster tool-path

Figure 5-21 shows the Coverage Area Map (*CAM*) for the ellipsoid with both the crowding effects, highlighted in green, and the unpolished envelope, highlighted in red. For an ellipsoid, the unpolished envelope and the crowding effect are both presents when the stepover size is maintained constant throughout the part surface.

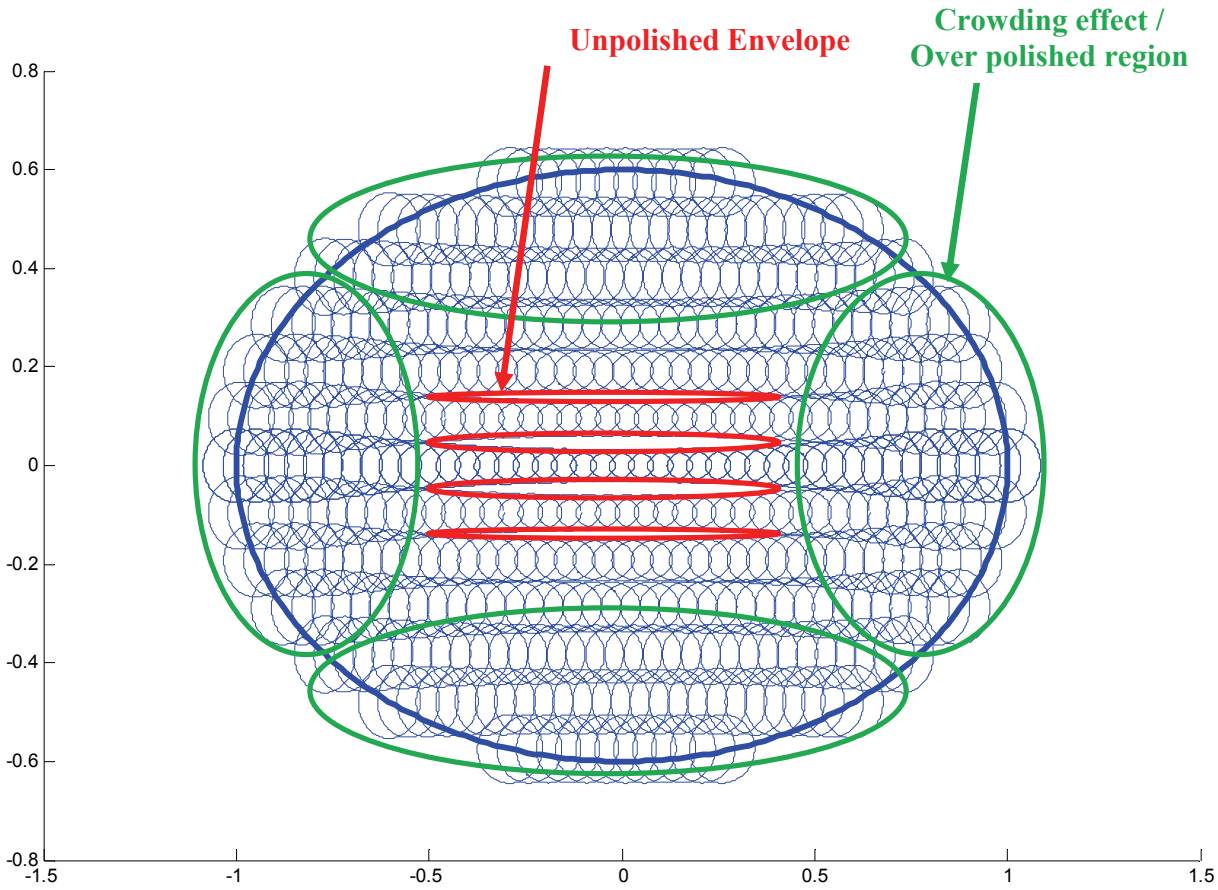

Figure 5-21: Crowding and unpolished areas for an ellipsoid

In conclusion, continuous raster path with constant stepover size results in unwanted effects during robotic polishing. The effects are crowding and under polishing as presented on the Coverage Area Map (*CAM*). Therefore, the polishing path must be modified to accommodate varying stepover size and guarantee full coverage area along the part surface. In the next chapter, an algorithm is developed to overcome these problems.

6 POLISHING PATH PLANNING

In Chapter 5 the Coverage Area Map (CAM) is utilized to show the contact area generated between the polishing tool and the part surface for three different parts. The *CAM* showed that for continuous raster path with constant stepover size two unwanted effects occurs depending on the stepover size. The problems are as follows:

1. Small stepover size resulted in crowding effect indicates that the polishing tool overlaps the same area more than once.
2. Large stepover size resulted in unpolished envelope indicates that the polishing tool does not come in contact with the part surface and implies that this envelope is not polished.

In the following chapter an algorithm is developed to overcome the problems identified in the continuous raster path with constant stepover size. The algorithm relies on the Coverage Area Map (*CAM*) to generate a tool-path that guarantees a full coverage area at the contact between the polishing tool and the part surface during the robotic polishing process.

The working procedure for computing the polishing path requires determination of the contact area at consecutive discrete contact points along the part surface. Once the contact area is determined for consecutive contact points, the modified polishing path is generated using the recursive method. To illustrate the idea, the Coverage Area Map (*CAM*) is utilized again and a set of mathematical expressions are generated to describe the full coverage area numerically.

6.1 Algorithm for generating polishing path

In the following section the algorithm for generating a polishing path that guarantees a full coverage area of the part surface is developed. Recall from Chapter 3 that the length of the contact area at any contact point N equals $2a_{ij}$ where a is the semi-major axis. To achieve a complete coverage area between two adjacent paths P_l and P_{l+1} the stepover size should have a maximum vertical distance of $2a_{il}$ between the centers of one contact area to adjacent one. Next,

representing $2a_{ij}$ as $[a_{ij} \quad a_{ij}]^T$ and substituting into Equation (4-7) results in the following symbolic equation for the Coverage Area Map (MAP):

$$CAM = \begin{Bmatrix} \begin{bmatrix} a_{10} \\ a_{10} \end{bmatrix} & \begin{bmatrix} a_{20} \\ a_{20} \end{bmatrix} & \cdots & \begin{bmatrix} a_{i0} \\ a_{i0} \end{bmatrix} \\ \begin{bmatrix} a_{11} \\ a_{11} \end{bmatrix} & \begin{bmatrix} a_{21} \\ a_{21} \end{bmatrix} & & \begin{bmatrix} a_{i1} \\ a_{i1} \end{bmatrix} \\ \begin{bmatrix} a_{12} \\ a_{12} \end{bmatrix} & \begin{bmatrix} a_{22} \\ a_{22} \end{bmatrix} & \cdots & \begin{bmatrix} a_{i2} \\ a_{i2} \end{bmatrix} \\ \vdots & \vdots & & \vdots \\ \begin{bmatrix} a_{1l} \\ a_{1l} \end{bmatrix} & \begin{bmatrix} a_{2l} \\ a_{2l} \end{bmatrix} & \vdots & \begin{bmatrix} a_{il} \\ a_{il} \end{bmatrix} \\ \vdots & \vdots & \ddots & \vdots \\ \begin{bmatrix} a_{1j} \\ a_{1j} \end{bmatrix} & \begin{bmatrix} a_{2j} \\ a_{2j} \end{bmatrix} & \cdots & \begin{bmatrix} a_{ij} \\ a_{ij} \end{bmatrix} \end{Bmatrix} \tag{6-1}$$

Note that $[a_{ij} \quad a_{ij}]^T$ represents the total length of the contact area at the i^{th} discretized point along the j^{th} polishing path. The Coverage Area Map (*CAM*) is plotted in Figure 6-1.

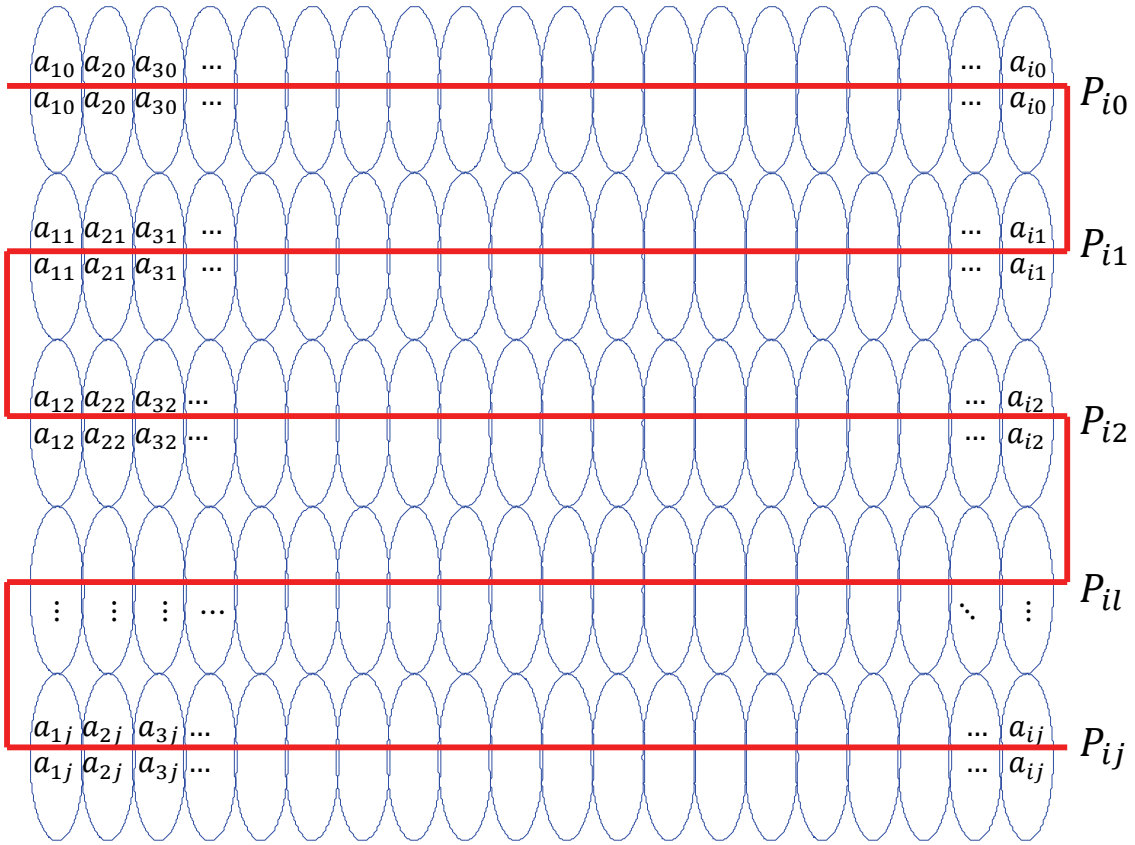

Figure 6-1: Coverage area map for modified polishing path

Up to this point the Coverage Area Map (*CAM*) has been generated and a mathematical expression has been developed to express the Coverage Area Map symbolically. Now, it is time to generate the algorithm for the modified polishing path based on the Coverage Area Map (*CAM*). The polishing path should address the following two issues:

1. Where to place the base path
2. Where to place adjacent paths

To start off, assume that the y position of each contact point is described by the following recursive equation:

$$\boldsymbol{P_{ij} = P_{ij-1} + a_{ij-1} + a_{ij}} \tag{6-2}$$

Next, define the base path as the first polishing path generated along the part surface ($i.e.\ j = 0$). The base pass P_{i0} is arbitrarily chosen along the part surface. Adjacent polishing path *i.e.* P_{i1} is generated relative to the base path. The position of the y axis for any polishing path is a function of the boundary of the semi-major axis a along the part surface. Therefore, the base path is also a function of y and is defined as follows:

$$P_{i0}(a_{i0}) = 0 \tag{6-3}$$

indicating that P_{i0} is a function of a_{i0} defined for the polishing path $j = 0$, and is assumed to be a straight line since it y position is 0; thus, it is ignored. The base path P_{i0} passes through the contact point N_{i0} at the center of the contact area CA_{i0} (*i.e.* along a_{i0} and not $2a_{i0}$). The y position of the next polishing path P_{i1} follows the recursive method as described by $P_{i1} = P_{i0} + a_{i0} + a_{i1}$. Where a_{i0} and a_{i1} are the semi-major axis of the first and second contact areas for the i^{th} element. Since, $P_{i0} = 0$ the equation reduces to

$$P_{i1} = a_{i0} + a_{i1} \tag{6-4}$$

All adjacent polishing paths along the part surface are described by the recursive method as follows:

$$\begin{aligned} P_{i2} &= P_{i1} + a_{i1} + a_{i2} \\ P_{i3} &= P_{i2} + a_{i2} + a_{i3} \\ &\vdots \\ P_{ij} &= P_{ij-1} + a_{ij-1} + a_{ij} \end{aligned} \tag{6-5}$$

This is a recursive method where determination of a polishing path requires the knowledge of the previous path. Alternatively, Equation (6-5) is written in the following form

$$\begin{Bmatrix} P_{i2} \\ P_{i3} \\ \vdots \\ P_{ij} \end{Bmatrix} = \begin{Bmatrix} a_{i0} + 2a_{i1} + a_{i2} \\ a_{i0} + \sum_{j=1}^{j=2} 2a_{ij} + a_{ij} \\ \vdots \\ a_{i0} + \sum_{j=1}^{j=j-1} 2a_{ij} + a_{ij} \end{Bmatrix} \tag{6-6}$$

Therefore, the contact points for the polishing path P_{ik} are placed at the y position of the path as defined by the following equation

$$P_{ij} = \begin{cases} 0 & j = 0 \\ a_{i0} + a_{ij} & j = 1 \\ a_{i0} + \sum_{j=1}^{j=j-1} 2a_{ij} + a_{ij} & j \geq 2 \end{cases} \tag{6-7}$$

Where P_{ij} is the j^{th} polishing path, a_{ij} is the semi-major axis of the contact area at the i^{th} element of the j^{th} polishing path. $\sum 2a_{ij}$ is a summation term of twice the semi-major axis.

The polishing path algorithm described by Equation (6-7) guarantees full coverage area during the robotic polishing process. The algorithm eliminates the crowding effects and the unpolished envelope identified in previous chapter. The algorithm reduces the vertical distance between two adjacent paths by summing up the semi-major axes of the contact area of each path.

In the next chapter, the parts that were analyzed in Chapter 4 are brought up again. The following algorithm is implemented into MATLAB software for numerical evaluation and the modified polishing tool path is generated.

7 MODIFIED POLISHING PATH

In the previous chapter an algorithm that guarantees full coverage area was developed. The algorithm is based on the recursive method where each polishing path depends on the previous path. The y position of contact point for the polishing path is the summation of the semi-major axes from all previous paths. In the following chapter the algorithm is applied to the three parts that were analyzed in previous chapter.

7.1 Part with two fixed radii of curvatures

Figure 7-1 shows the modified Coverage Area Map for the flat surface where the stepover size was defined according to the algorithm developed in Chapter 6. In this case the modified *CAM* shows a full coverage of the part surface. The stepover size between each polishing path is determined by summing up the y positions of the semi-major axis a. Since this is a special case for the *CAM* the stepover size between two adjacent paths remained uniform throughout the part surface. This is a result of uniform contact area as predicted in prior analysis.

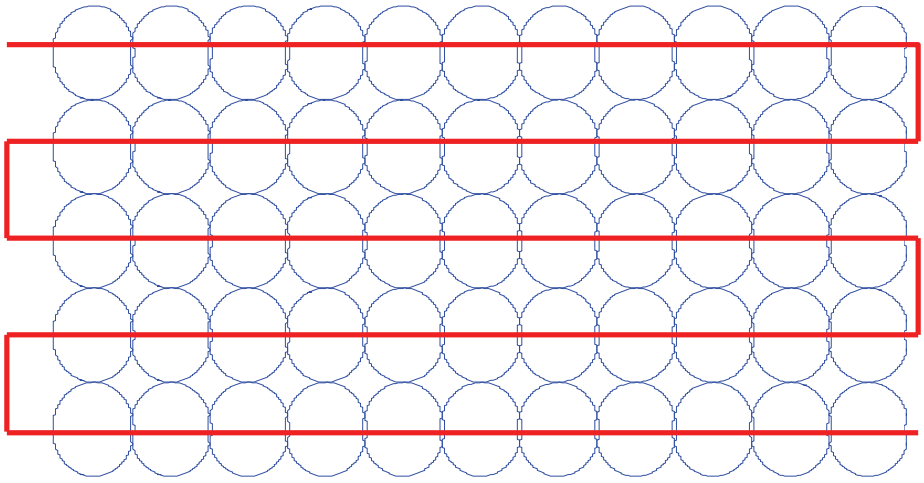

Figure 7-1: Modified polishing path for a flat surface

For flat surfaces the stepover size is constant between adjacent paths and the computation is relatively easy. The following example is more involved and generates interesting results.

7.2 Part with one fixed and one changing radii of curvatures

Figure 7-2shows the modified Coverage Area Map for the semi-spherical part surface where the stepover size was defined according to the algorithm developed in Chapter 6. In this case the modified *CAM* shows a full coverage of the part surface. The stepover size between each polishing path is determined by summing up the y positions of the semi-major axis a. Notice that a small overlap is generated between two adjacent paths. This slight overlap is desired to compensate for imperfections in the polishing tool.

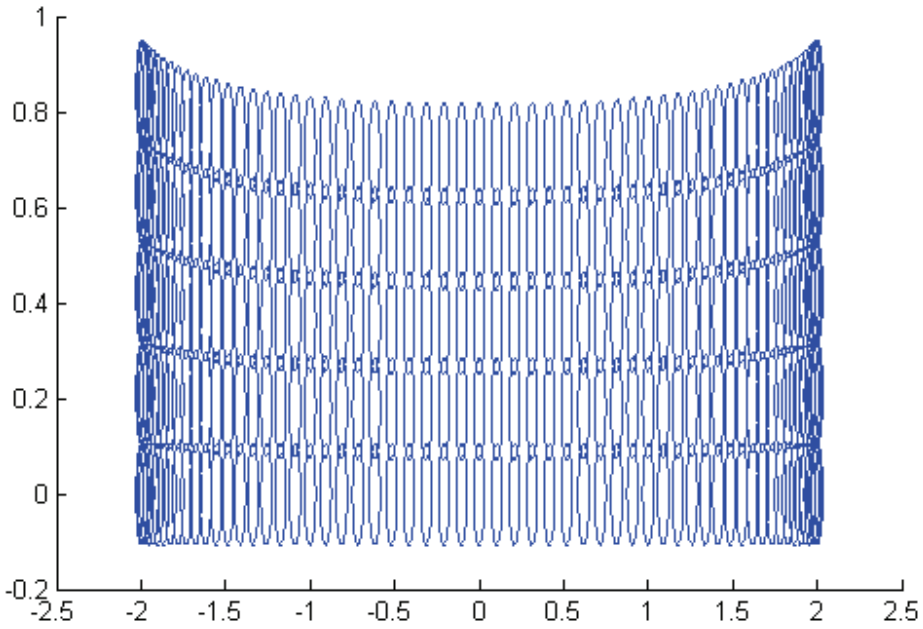

Figure 7-2: Modified *CAM* for semi-spherical part surface

Figure 7-3 shows the modified polishing path for the semi-spherical part surface. Note that the base polishing path is a straight line since that in Chapter 6 the y position of this path is defined to be at $P_0(a_{i0}) = 0$. Adjacent paths are summation of the semi-major axis generated at the contact points between the polishing tool and the part surface. Notice that the path becomes more curved for each polishing path. The figure shows that both the crowding effects and the unpolished area were eliminated along the part surface.

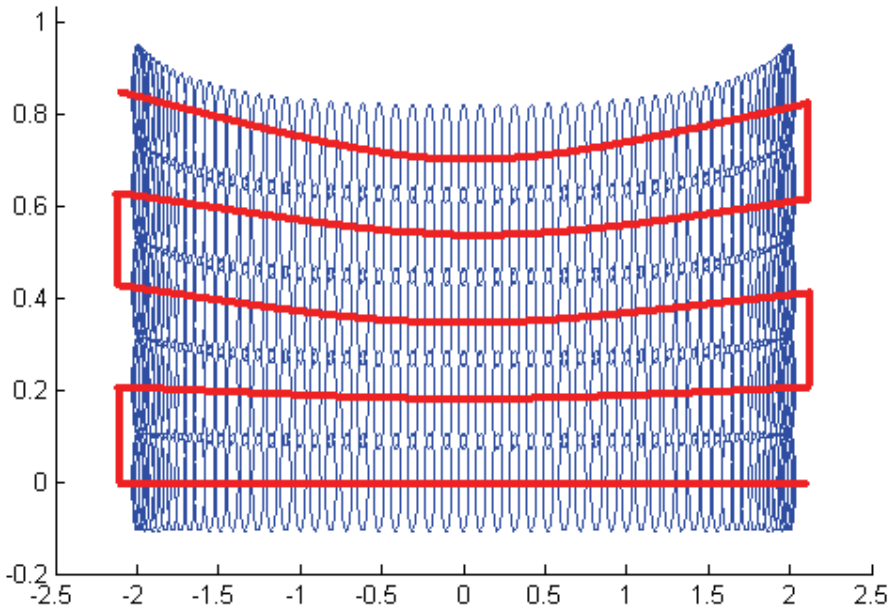

Figure 7-3: Modified polishing path for semi-spherical part

Figure 7-4 shows an unpolished area, highlighted in red, generated at the end of the path. Therefore the unpolished area was not completely eliminated but is pushed away to the end of the polishing path.

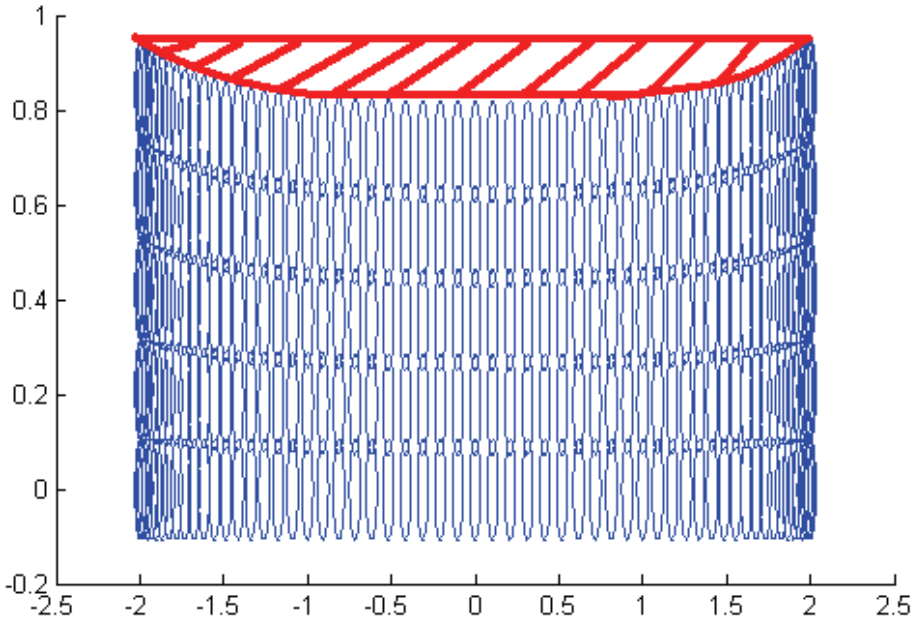

Figure 7-4: Unpolished area on the modified polishing path

7.3 Part with two changing radii of curvatures

Figure 7-5 shows the modified Coverage Area Map (*CAM*) for the ellipsoid where the stepover size was defined according to the algorithm developed in Chapter 6. In this case the modified *CAM* shows a full coverage along the part surface. The stepover size between each polishing path is determined by summing up the y positions of the semi-major axis a. Recall that because of the geometrical complexity of the problem, the part surface was divided into two separate sections. The Coverage Area Map (*CAM*) was generated for each section separately and then it is combined.

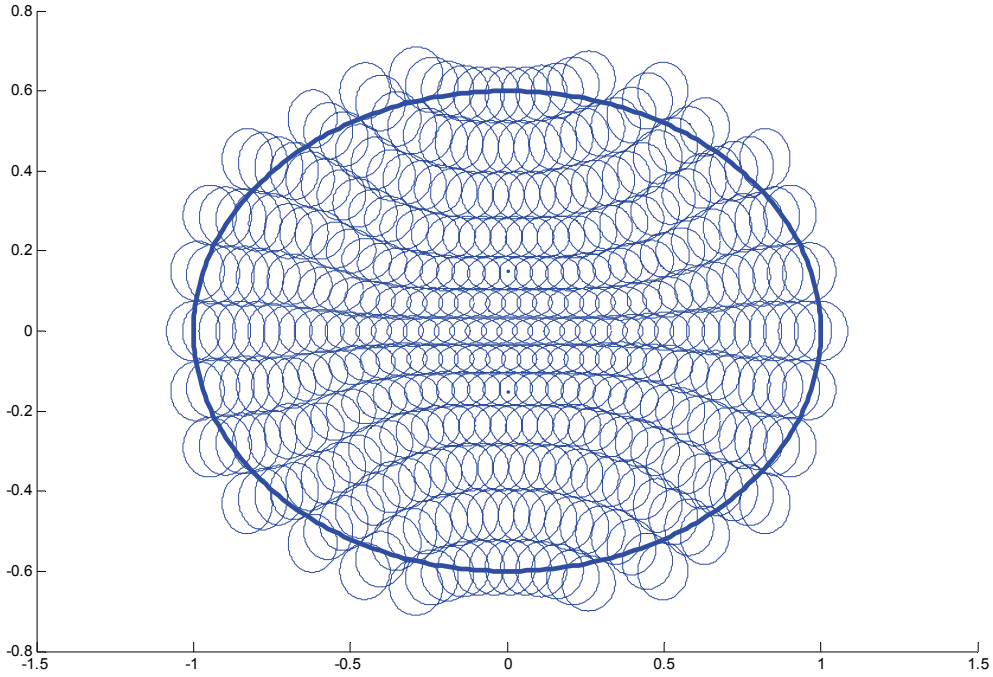

Figure 7-5: Modified *CAM* for ellipsoid

The base path was defined to be at $y = 0$ therefore it is a straight line. There is symmetry along the x axis since that the part surface was divided into two separate sections and the (*CAM*) was generated for each section separately and then combined into one figure.

Figure 7-6 shows the modified polishing path for the ellipsoid where the radii of curvatures changes in both xz and yz planes for every discretized contact point. Exact results for the polishing path were not obtained for the ellipsoid during this research due to time limitation. Therefore an approximated polishing path is given here.

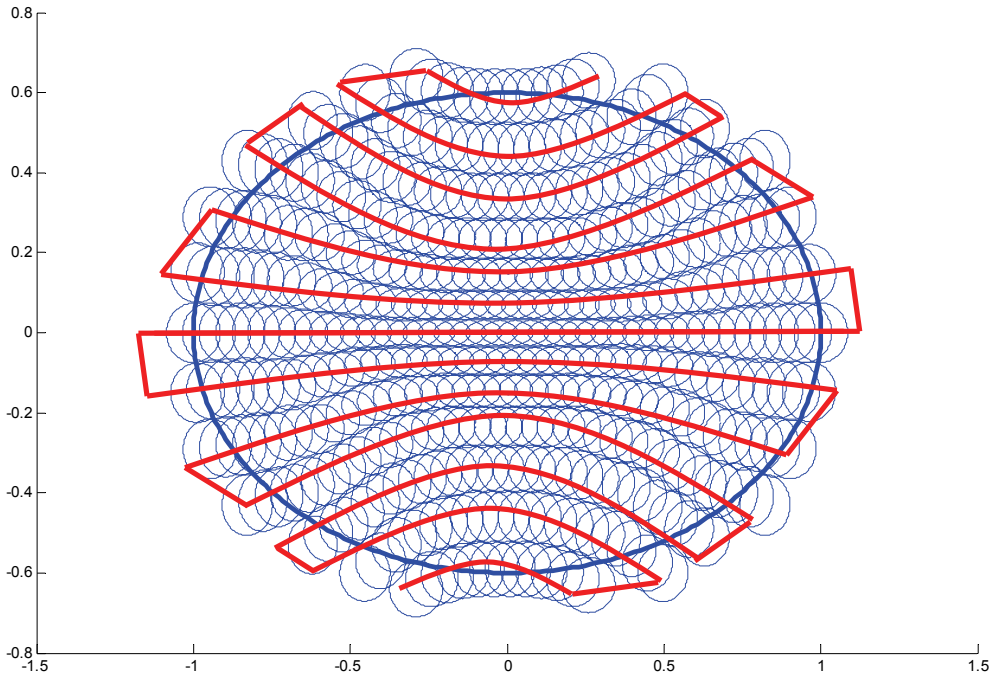

Figure 7-6: Modified polishing path for ellipsoid

Here is a brief explanation why exact polishing path was not obtained and an approximated path is generated instead:

For the case of a flat surface the radii of curvatures of the part surface approaches infinity and the contact area is circular throughout the polishing path. Therefore, the semi-major axis a_{ik} of any contact point always equals the semi-major axis of adjacent contact point a_{ik+1}. The radii of curvatures of the part surface are constants along the pat surface. Therefore, changing the y position of any contact point does not affect the contact area. The modified polishing path is generated according to the algorithm developed in Chapter 6.

The same is true for the second part surface where the radius of curvature changes along the x axis but maintained constant along the y axis. Since the radius of curvature is constant along the y axis, changing the y position of any contact point will not affect the contact area. Therefore the modified polishing path is generated using the algorithm developed in Chapter 6.

For the case where both radii of curvatures change along the part surface the modified polishing path is complicated to generate and the recursive method still applies, but small modification is required. The complication arises since the radius of curvature constantly changes in the xz and yz planes. Both planes are functions of x, y and z axes. Changing the x or y positions of a contact point changes the z position of the contact point. Therefore, the radius of curvature changes which results in different contact area. Figure 7-7 shows a wire frame design of the part surface. Note that changing the position of the contact point from point 1 to point 2, changes the z position of the part surface which results in different radius of curvature. Thus, changing the position of the contact points result in different coverage area.

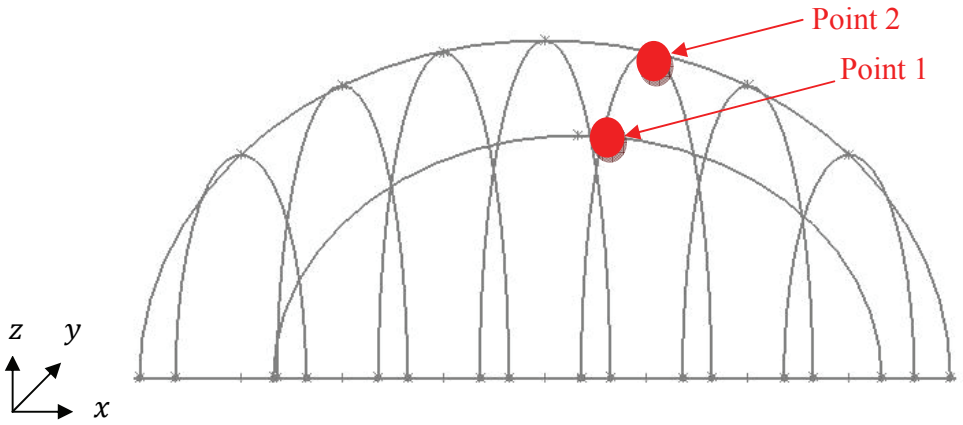

Figure 7-7: Wire frame design of an ellipsoid

To generate the modified polishing path that guarantees full coverage area an iterative search method has to be implemented for the recursive method. The search method calculates the semi-major axis a_{ij+1} at a given contact point and adopt itself to the previous semi-major axis a_{ij} until there is no crowding effect or unpolished regions along the part surface.

In conclusion, the following chapter showed the Coverage Area Map (*CAM*) for the modified polishing path using the recursive algorithm developed in Chapter 6. It was shown that the algorithm guarantees full coverage area of the part surface during robotic polishing. Three part surface were analyzed:

1) 2 fixed radii of curvatures (i.e. flat surfaces)
2) 1 fixed radius of curvature + 1 varies along the part surface (i.e. semi-spherical tube)
3) 2 varying radii of curvatures (i.e. ellipsoid)

Full coverage area is obtained for the first two cases and the number of polishing path is reduced. Crowding effects and unpolished regions were eliminated and full coverage area is obtained by implementing the exact algorithm developed in Chapter 6. However, for the third case an approximation method is implemented and subsequent research is required. Elaborated discussion is provided as to why an approximation method is used and how to solve the problem.

8 CONCLUSIONS AND FUTURE WORK

Based on the method introduces in this thesis, a modified polishing path is developed for automated polishing process. Summarized in the following are the major contributions:

- A model for the contact area generated between the polishing tool and the part surface is developed. The model is based on Hertzian contact theory as developed in the branch of contact mechanics. Contact area refers to the area generated between two separate non-conforming bodies made of elastic materials under applied compressive force P.
- A theory for generating a Coverage Area Map (*CAM*) was developed. The Coverage Area Map is a two dimensional map that shows the contact area generated between the polishing tool and the part surface during robotic polishing process. The theory requires a series of contact points to be defined along the part surface and used to develop a continuous polishing path with constant stepover size. The *CAM* theory is applied for a single discontinued raster path and a continuous raster path with constant stepover size.
- The Coverage Area Map showed that constant stepover size between polishing paths does not guarantee a full coverage of the part surface. The problems associated with constant polishing paths included under-polishing and over-polishing of the part surface.
- An Algorithm that guarantees full coverage area during the polishing process has been developed. The algorithm relies on the continuous raster path.
- The polishing path has been modifies according to the algorithm developed. For the modified path the stepover size has been determined based on previous paths. In was shown that modified path guarantees a full coverage of the part surface.
- The Coverage Area Map and the modified polishing path were tested on three different part surfaces and results were provided in diagrams.

The focus of this work is to generate a polishing path that guarantees full coverage area during polishing. The Coverage Area Map (*CAM*) was generated for three unique part surfaces. The method developed herein is proved to be efficient and guarantees full coverage of the part

surface. However, future work is required. Here is a list of recommended work required to improve the algorithm presented:

- The polishing tool in the proposed algorithm is assumed to be normal to the part surface at all time. In practical terms this is not realistic because of the nature of the problem. To improve the algorithm, a method that accommodates angle change of the tool along the part surface has to be incorporated.
- It was shown that for a flat surface the radii of curvatures of the part surface approaches infinity and the contact area is circular throughout the polishing path. Therefore, changing the y position of any contact point does not affect the contact area. The same is true for the second part where the radius of curvature changes along the x axis but maintained constant along the y axis. The radius of curvature in this case is also constant along the y axis; changing the y position of any contact point will not affect the contact area. For the third case where both radii of curvatures change along the part surface the modified polishing a complication arises since that the radius of curvature constantly changes in the xz and yz planes. Therefore, changing the x or y positions of a contact point changes the z position of the contact point. In this case, the radius of curvature changes which results in different contact area. Thus the algorithm developed here has to be modified and include a search method that calculated the contact area at each point as it moves along the surface.
- The following work did not take into consideration the micro cutting model for polishing but is solely based on macro polishing model. Future work will have to incorporate both models to achieve realistic polishing model.

9 REFERENCES

1. **Tam, Hon-Yuen and Cheng, Haobo.** An investigation of the effect of the tool path on the removal of material in polishing. *Journal of Material Processing Technology.* 2010, pp. 807-818.

2. **S., Malkin.** *Grinding Technology: Theory and Applications of Machining with Abrasives.*

3. **Liao, Liang.** *Modelling and Control of Automated Polishing/Deburring Process.* PhD dissertation : Department of Aerospace Engineering, Ryerson University. 2008.

4. **Lambie, James.** *Design and optimization of CNC based polishing process.* MASc thesis : Department of Aerospace Engineering, Ryerson University. 2008.

5. **Ahn, J.H., et al.** Intelligently automated polishing for high quality surface formation of sculptured die. *Journal of Materials Processing Technology.* 2002, Vols. 130–131, 339–344.

6. **Guvenc, L. and Srinivasan, K.** An Overview of Robot-Assisted Die and Mold Polishing with Empasis on Process Modelling. *Journal of Manufacturing Systems.* Vol. 16 No. 1, 1997, pg. 49.

7. **Tsai, M.J. and Huang, J.F.** Efficient Automatic Polishing Process with a New Compliant Abresive Tool. *International Journal of Advanced Manufacturing Technology.* 2006, Vol. 30, pp. 817-827.

8. **Dragomatz, D and Mann, S.** A classified bibliography of literature on NC milling path generation. *Comput-Aided Design.* 1997, Vol. 29, (3) Page: 239-247.

9. **Sciavicco, Lorenzo and Siciliano, Bruno.** *Modelling and Control of Robot Manipulator.* Great Britian : Springer-Verlag London Limited, 2005. ISBN: 1-85233-221-2.

10. **Misra, Debananda, Sundararajan, V. and Wright, Paul K.** Zig-Zag Tool Path Generation for Sculptured Surface Finishing. Department of Mechanical Engineering, University of California, Berkeley, CA, USA.

11. Consortium for Research and Inovation in Aerospace in Quebec (CRAIQ). *http://www.criaq.aero/.* [Online]

12. **Groover, Mikell P.** *Fundumentals of Modern Manufacturing: Materials, Processes, and systems Ed. 3.* pg. 594 - 617 : John Wiley & Sons, Inc., 2007. ISBN: 978-0-471-74485-6.

13. **Avery, Roswell.** *Modelling for Contact Stress Control in Automated Polishing.* Department of Mechanical Engineering, Ryerson University : MASc Thesis Report, 2004.

14. **Tsai, M.J., Huang, J.F. and Kao, W.L.** Robotic polishing of precision molds with uniform material removal control. *InternationalJournalofMachineTools&Manufacture.* 49, 2009, Vols. page 885–895.

15. **Wang, Guilian Wang and Yiqiang.** Research on polishing process of a special polishing machine tool. *Machining Science and Technology.* 2009, Vol. 13, pp. 106–121.

16. **Liang Liao, Fengfeng Xi, and Guanjian Liu.** Adaptive Control of Pressure Tracking for Polishing Process. *ASME Journal of Manufacturing Science and Engineering.* April 2010.

17. **Y. Mizugaki, M. Sakamoto, and H. Ikuta,.** Experimental optimization of mold machining conditions in a model-based polishing robot system. *24th International Symposium on Industrial Robots.* 1993, pp. 43-48.

18. **Y. Takeuchi, N. Askawa, and D.F. Ge,.** Automation of polishing work by an industrial robot. *JSME Int. J. Ser. .* 36, 1993, Vol. 4, pp. 556-561.

19. **Furukawa, T., Rye, D.C. and Dissanayake, M.W.M.G. and Barratt, A.J.** Automated polishing of an unknown three-dimensional surface. *Robotics & Computer-Integrated Manufacturing.* 12, 1996, Vol. 3, pp. 261-270.

20. **Avery Roswell, Fengfeng Xi, and Guanjian Liu.** Modelling and analysis if stress for automated polishing. *International Journal of Machine Tools & Manufacturing.* 2006, Vol. 46, pp. 424-435.

21. **Liao, Liang and Xi, Fengfeng.** A Linearized Model for Control of Automated Polishing Process. *In Proceeding of 2005 IEEE Conference Control Application.* Toronto, Canada, August 28-31, 2005.

22. **Dragomatz, D. and Mann, S.** A Classified Bibliography of Literature on NC Tool Path Generation. *Computer-Aided Design.* March 1997, Vol. 29, No. 3.

23. **Toh, C.K.** A study of the effects of cutter path strategies and orientations in milling. *Journal of Material Processing Technoology.* 2004, Vol. 152, pp. 346-356.

24. **Kim, Hyun-Chul.** Tool path generation for contour parallel milling with incomplete mesh model. *The International Journal of Advanced Manufacturing Technology.* 2010, Vol. 48, 5-8 pp. 443-454, DOI: 10.1007/s00170-008-1733-9 .

25. **Yao, Zhiyang.** A Novel Cutter Path Planning Approach to High Speed Machining. *Chinese University of Hong Kong.* email: zyyao@acae.cuhk.edu.hk.

26. **Topal, E.S.** The roll of stepover ration in prediction of surface roughness in flat end milling. *International Journal of Mechanical Science.* 2009, Vol. 51, pp. 782-789.

27. **Lo, C-C.** Efficient cutter-path planning for five-axis surface machining with a flat-end cutter. *Computer-Aided Design.Vol.* 31, 1999, pp. 557–566.

28. **Choi, Young Keun.** *Tool path generation and 3D tolerenceanalysis for free-form surfaces.* Department of Industrial Engineering, Texas A&M University : PhD dissertation, 2004.

29. **Wei He, Ming Lei and Hongzan Bin.** Iso-parametric CNC tool path optimization based on adaptive grid generation. *International Journal in Advanecd Manufacturing Technology.* 2009, Vols. 41, pp. 538–548, DOI 10.1007/s00170-008-1500-y.

30. **Grievey, A. Hatnay and B.** Cartesian machining versus parametric machining: a comparative study. *International journal of production research.* 2000, Vol. 38, 13, pp. 3043-3065.

31. **Choen, Gershon Elber and Elaine.** Toolpath generation for freeform surface models. *Computer-Aided Design.* 26, 1994, Vol. 6, pp. 490-496.

32. **Li, Hsi-Yung Deng and Huiwen.** Constant scallop-height tool path generation for 3 axis machining. *Computer-Aided Design.* 34, 2002, pp. 647-654.

33. Fundamental issues in tool path planning. *Advanced Numerical Methods to Optimize Cutting Conditions of five-axis Machining.* DOI: 10.1007/978-3-540-71121-6_3 : Springer Series in Advanced Manufacturing, 2007.

34. **Oliveria, Joa˜ O Batista.** Robust approximation of offsets, bisectors, and medial axes of plane curves. *Reliable Computing* . 2003, Vol. 9, pp. 161–175.

35. **Neff, R.T. Farouki and C.A.** 1990 Analytic properties of plane offset curves. *Computer Aided Geometric Design.* 1990, Vol. 7, pp. 83-99.

36. **Duc, Christophe Tournier and Emmanuel.** Iso-scallop tool path generation in 5-axis milling. *International Journal of Advanced Manufacturing Technology.* 2005, Vol.25, pp. 867–875, DOI 10.1007/s00170-003-2054-7.

37. **Wang, Nan and Tang, Kai.** Five axis tool path generation for a flat-end tool based on iso-conic partitioning. *Computer-Aided Design.* 2008, Vol. 40, Page 1067-1079.

38. **Jun C.S., Cha K. and Lee Y.S.** Tool orientations for 5-axis machining by configuration-space search method. *Computer-Aided Design.* 2003, Vol. 35, 6.

39. **Lee, Yuan-Shin.** Non-Isoparametric tool path planning by machining strip evaluation ofr 5-axis sculptured surface machining. *Computer-Aided Design.* 1998, Vol. 30, 7.

40. **Hon-yuen Tam, Osmond Chi-hang Lui, and Alberet C.K. Mok.** Robotic polishing of free-form surfaces using scanning paths. *Journal of Materials Processing Technology.* 1995, Vol. 95, pp. 191-200.

41. **K.L., Johnson.** *Contact Mechanics.* The Pitt Building, Trumpington St. : Cambridge University Press, 1989. 84-11349.

42. **Wang, H. Wu and J. M.** Non-Hertzian conformal contact at wheel / rail interface. *in Proceedings of the IEEE/ASME Joint Railroad Conference, Baltimore, MD.* 1995, pp. 137-144.

43. **Boresi, A.P., Schmidt, R.J. and Sidebottom, O.M.** *Advanced Mechanics of Materials.* s.l. : John Wiley & Sons, Inc., 1993. 5th Ed..

44. **Basanez, Luis and Rosell, Jan.** Robotic Polishing Systems from Graphical Task Specification to Automatic Programming. *IEEE Robotics & Automation Magazine.* September 2005, pp. 35-43.

45. **Sciavicco, Lorenzo and Siciliano, Bruno.** *Modelling and Control of Robot Manipulator.* Great Britian : Springer-Verlag London Limited, 2005.

46. **Durcy, Gerard.** Manual Polishing Operations Carried Out On Parts Fixed In a Rotating Tool. November 24, 2006.

48. **Lambie, James.** *Design and optimization of CNC based polishing process.* MASc thesis : Ryerson University, Department of Aerospace Engineering. 2008.

49. **Takeuchi, Yoshimi, Ge, Dongfang and Asakawa, Naoki.** Automated Polishing Process with a Human-like Dexterous Robot. 1993, Vol. 3, DOI: 10.1109/ROBOT.1993.292266, pp. 950 - 956.

50. **K. Tang, S.Y. Chou and L.L. Chen.** An algorithm for reducing tool retractions in zigzag pocket machining. *Computer-Aided Design.* 1998, Vol. 30, 2.

51. **Durcy, Gerard.** Manual Polishing Operations Carried Out On Parts Fixed In a Rotating Tool. November 24, 2006.

52. **Guvenc, L. and Srinivasan, K.** An Overview of Robot-Assisted Die and Mold Polishing with Empasis on Process Modelling. *Journal of Manufacturing.* 1997, Vol. 16, 1.

10 APPENDIX A

Equation of an ellipsoid:

The equation of ellipsoid aligned at the origin of xyz Cartesian coordinate system is given by:

$$\frac{x^2}{a^2}+\frac{y^2}{b^2}+\frac{z^2}{c^2}=1 \tag{A-1}$$

where a, b and c are fixed positive real numbers that determine the shape of the ellipsoid.

Rearranging (1)

$$\frac{x^2}{a^2}+\frac{z^2}{c^2}=1-\frac{y^2}{b^2} \tag{A-2}$$

Dividing both sides by $\frac{b^2-y^2}{b^2}$ leads to the following equation

$$\frac{x^2}{\left[\frac{a^2(b^2-y^2)}{b^2}\right]}+\frac{z^2}{\left[\frac{c^2(b^2-y^2)}{b^2}\right]}=1 \tag{A-3}$$

By letting $A_{xz}=\left[\frac{a^2(b^2-y^2)}{b^2}\right]$ and $C_{xz}=\left[\frac{c^2(b^2-y^2)}{b^2}\right]$ the equation of an ellipsoid in the XZ plane can now be expresses as:

$$\frac{x^2}{A_{xz}}+\frac{z^2}{C_{xz}}=1 \tag{A-4}$$

In the same way the equation of an ellipsoid in the YZ plane is given by

$$\frac{y^2}{B}+\frac{z^2}{C_{yz}}=1 \tag{A-5}$$

Where $A_{yz}=\left[\frac{b^2(a^2-x^2)}{a^2}\right]$ and $C_{yz}=\left[\frac{c^2(a^2-x^2)}{a^2}\right]$.

Radius of curvature

The radius of curvature for the ellipsoid can be generated by manipulating the equation of curvature of an ellipse in two different planes. The equation of curvature of an ellipse in the xy plane is given by:

$$K_{xy}=\frac{x'y''-y'x''}{\left(x'^2+y'^2\right)^{\frac{3}{2}}} \tag{A-6}$$

Where $x=a\,cos\,(\theta)$, $y=b\,sin\,(\theta)$ and x', x'', y' and y'' are the first and second derivatives of x and y.

To calculate the radius of curvature in the xz plane let

$$K_{xz} = \frac{x'z'' - z'x''}{\left(x'^2 + z'^2\right)^{\frac{3}{2}}} \tag{A-7}$$

This is simplified to

$$K_{xz} = \frac{AC_{xz}}{\left(A^2\left(\frac{z^2}{c^2}\right) + C_{xz}^2\left(\frac{x^2}{a^2}\right)\right)^{\frac{3}{2}}} \tag{A-8}$$

To calculate the radius of curvature in the yz plane let

$$K_{yz} = \frac{y'z'' - z'y''}{\left(y'^2 + z'^2\right)^{\frac{3}{2}}} \tag{A-9}$$

This is simplified to

$$K_{yz} = \frac{BC_{yz}}{\left(B^2\left(\frac{z^2}{c^2}\right) + C_{yz}^2\left(\frac{x^2}{b^2}\right)\right)^{\frac{3}{2}}} \tag{A-10}$$